Low-Latency Multiuser Two-Way Wireless Relaying for Spectral and Energy Efficiencies

Sheng , Z., Tuan, H. D., Duong, Q., Poor, H. V., & Fang, Y. (2018). Low-Latency Multiuser Two-Way Wireless Relaying for Spectral and Energy Efficiencies. *IEEE Transactions on Signal Processing*, *66*(16), 4362-4376. https://doi.org/10.1109/TSP.2018.2847626

Published in:
IEEE Transactions on Signal Processing

Document Version:
Peer reviewed version

Queen's University Belfast - Research Portal:
Link to publication record in Queen's University Belfast Research Portal

Publisher rights
© 2018 IEEE. This work is made available online in accordance with the publisher's policies. Please refer to any applicable terms of use of the publisher.

General rights
Copyright for the publications made accessible via the Queen's University Belfast Research Portal is retained by the author(s) and / or other copyright owners and it is a condition of accessing these publications that users recognise and abide by the legal requirements associated with these rights.

Take down policy
The Research Portal is Queen's institutional repository that provides access to Queen's research output. Every effort has been made to ensure that content in the Research Portal does not infringe any person's rights, or applicable UK laws. If you discover content in the Research Portal that you believe breaches copyright or violates any law, please contact openaccess@qub.ac.uk.

Download date:04. May. 2023

Low-Latency Multiuser Two-Way Wireless Relaying for Spectral and Energy Efficiencies

Z. Sheng, H. D. Tuan, T. Q. Duong, H. V. Poor, and Y. Fang

***Abstract*—The paper considers two possible approaches, which enable multiple pairs of users to exchange information via multiple multi-antenna relays within one time-slot to save the communication bandwidth in low-latency communications. The first approach is to deploy full-duplexes for both users and relays to make their simultaneous signal transmission and reception possible. In the second approach, the users use a fraction of a time slot to send their information to the relays and the relays use the remaining complementary fraction of the time slot to send the beamformed signals to the users. The inherent loop self-interference in the duplexes and inter-full-duplexing-user interference in the first approach are absent in the second approach. Under both these approaches, the joint users' power allocation and relays' beamformers to either optimize the users' exchange of information or maximize the energy-efficiency subject to user quality-of-service (QoS) in terms of the exchanging information throughput thresholds lead to complex nonconvex optimization problems. Path-following algorithms are developed for their computational solutions. The provided numerical examples show the advantages of the second approach over the first approach.**

***Index Terms*—Full-duplex, time-fraction allocation, relay beamforming, power allocation, spectral efficiency, energy efficiency, multi-user communication, path-following methods**

I. Introduction

Full-duplexing (FD) [1]–[5] is a technique for simultaneous transmission and reception in the same time slot and over the same frequency band while two-way relaying (TWR) [6]–[9] allows pairs of users to exchange their information in one step. FD deployed at both users and relays thus enables the users to exchange information via relays within a single time-slot [10]. This is in contrast to the conventional one-way relaying which needs four time slots, and the half-duplexing (HD) TWR [8], [11]–[13], which needs two time slots for the same task. Thus, FD TWR seems to be a very attractive tool for device-to-device (D2D) and machine-to-machine (M2M) communications [14], [15] and low latency communication [16]–[18] for Internet of Things (IoT) applications.

The major issue in FD is the loop self-interference (SI) due to the co-location of transmit antennas and receive antennas. Despite considerable progress [3]–[5], it is still challenging to attenuate the FD SI to a level such that FD can use techniques of signal processing to outperform the conventional half-duplexing in terms of spectral and energy efficiencies [19], [20]. Similarly, it is not easy to manage TWR multi-channel interference, which becomes double as compared to one-way relaying [21], [22]. The FD-based TWR suffers even more severe interference than the FD one-way relaying, which may reduce any throughput gain achieved by using fewer time slots [10].

There is another approach to implement half-duplexing (HD) TWR within a single time slot, which avoids FD at both users and relays. In a fraction of a time slot, the HD users send the information intended for their partners to the relays and then the relays send the beamformed signals to the users within the remaining fraction of the time slot. In contrast to FD relays, which use half of their available antennas for simultaneous transmission and reception, the HD relays now can use all their antennas for separate transmissions and receptions. Thus, compared with FD users, which need two antennas for simultaneous transmission and reception, the HD users now need only one antenna for separate transmission and reception.

In this paper, we consider the problem of joint design of users' power allocation and relays' beamformers to either maximize the user exchange information throughput or the network energy efficiency [23] subject to user quality-of-service (QoS) constraints in terms of minimal rate thresholds. As they constitute optimization of nonconvex objective functions subject to nonconvex constraints under both these approaches, finding a feasible point is already challenging computationally. Nevertheless, like [13] we develop efficient path-following algorithms for their computation, which not only converge rapidly but also invoke a low-complexity convex quadratic optimization problem at each iteration for generating a new and better feasible point. The numerical examples demonstrate the full advantage of the second approach over the first approach. Some transformations proposed in [13] to transform nonconvex constraints to convex constraints for computational tractability are also used in this paper. However, compared to [13] the paper offers the following further developments:

- To address the optimization problems in an FD-based TWR setting, we propose a new and tighter bound for the nonconcave objective functions, which is based on one step of approximation instead of multiple steps of approximation in [13]. This helps to expand the search area for locating an optimal solution to accelerate the computational convergence.
- The presence of time fractions as an additional opti-

This work was supported in part by a U.K. Royal Academy of Engineering Research Fellowship under Grant RF1415/14/22, and in part by the U.S. National Science Foundation Grants CNS-1702808 and ECCS-1647198.

Zhichao Sheng and Hoang D. Tuan are with the school of Electrical and Data Engineering, University of Technology Sydney, Broadway, NSW 2007, Australia (email: zhichaosheng@163.com, Tuan.Hoang@uts.edu.au)

Trung Q. Duong is with Queen's University Belfast, Belfast BT7 1NN, UK (email: trung.q.duong@qub.ac.uk)

H. Vincent Poor is with the Department of Electrical Engineering, Princeton University, Princeton, NJ 08544, USA (email: poor@princeton.edu)

Yong Fang is with the School of Communication and Information Engineering, Shanghai University, Shanghai, China (email: yfang@staff.shu.edu.cn)

mization variable in the optimization problems in TF-wise HD TWR setting makes the transformations proposed in [13] no longer sufficient for transforming all nonconvex constraints to convex constraints. We develop new complementary transformations for transforming the nonconvex-still constraints to convex constraints, preserving the convexity of the existing convex constraints and making the objective functions more computationally tractable. Novel lower bounding approximations for the new objective functions, which are based on newly obtained inequalities, are then derived for developing the corresponding efficient path-following algorithms.

The rest of this paper is organized as follows. Section II considers the two aforementioned nonconvex problems under a FD-based TWR setting. Section III considers them under the time-fraction (TF)-wise HD TWR setting. Section IV verifies the full advantage of the TF-wise HD TWR over FD-based TWR via numerical examples. Section V concludes the paper. The appendix provides some fundamental inequalities, which play a crucial role in the development of the path-following algorithms in the previous sections.

Notation. Bold-faced characters denote matrices and column vectors, with upper case used for the former and lower case for the latter. $\boldsymbol{X}(n,\cdot)$ represents the nth row of the matrix $\boldsymbol{X}$ while $\boldsymbol{X}(n,m)$ is its (n,m)th entry. $\langle \boldsymbol{X} \rangle$ is the trace of the matrix $\boldsymbol{X}$. $(.)^T$ and $(.)^H$ respectively are the transpose and complex transpose operators. The inner product between vectors $\boldsymbol{x}$ and $\boldsymbol{y}$ is defined as $\langle \boldsymbol{x}, \boldsymbol{y} \rangle = \boldsymbol{x}^H \boldsymbol{y}$. $||.||$ is referred either to the Euclidean vector squared norm or the Frobenius matrix squared norm. Accordingly, $||\boldsymbol{X}||^2 = \langle \boldsymbol{X}^H \boldsymbol{X} \rangle$ for any complex $\boldsymbol{X}$. Lastly, $\boldsymbol{x} \sim \mathcal{CN}(\bar{\boldsymbol{x}}, \boldsymbol{R}_{\boldsymbol{x}})$ means $\boldsymbol{x}$ is a vector of Gaussian random variables with mean $\bar{\boldsymbol{x}}$ and covariance $\boldsymbol{R}_{\boldsymbol{x}}$.

II. Full-duplexing based two-way relaying

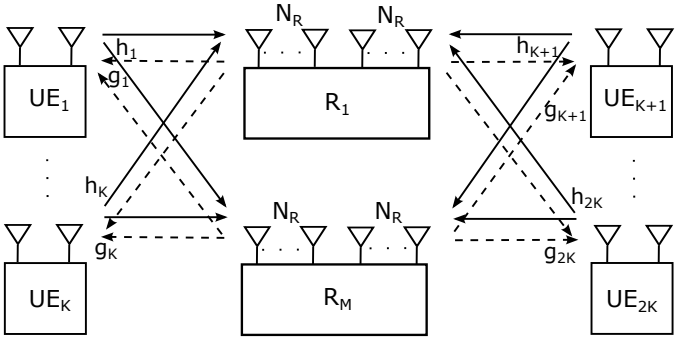

Fig. 1. Two-way relay networks with multiple two-antenna users and multiple multi-antenna relays.

Fig. 1 illustrates a FD TWR network consisting of K pairs of FD users (UEs) and M FD relays indexed by $m \in \mathcal{M} \triangleq \{1,\ldots,M\}$. Each FD user (UE) uses one transmit antenna and one receive antenna, while each FD relay uses N_R receive antennas and N_R transmit antennas. Without loss of generality, the kth UE (UE k) and $(k+K)$th UE (UE $k+K$) are assumed to exchange information with each other via the relays. The pairing operator is thus defined as $a(k) = K + k$ for $k \leq K$ and $a(k) = k - K$ if $k > K$. For each $k \in \mathcal{K} \triangleq \{1,\ldots,2K\}$, define the set of UEs, which are in the same side with kth UE as

$$\mathcal{U}(k) = \begin{cases} 1,2,...,K & \text{for} \quad 1 \leq k \leq K \\ K+1,...,2K & \text{for} \quad k \geq K+1. \end{cases}$$

Under simultaneous transmission and reception, FD UEs in $\mathcal{U}(k)$ interfere each other. Such kind of interference is called inter-FD-user interference.

Let $\boldsymbol{s} = [s_1,\ldots,s_{2K}] \in \mathcal{C}^{2K}$ be the vectors of information symbols s_k transmitted from UEs, which are independent and have unit energy, i.e. $\mathbb{E}[\boldsymbol{s}\boldsymbol{s}^H] = \boldsymbol{I}_{2K}$. For $\boldsymbol{h}_{\ell,m} \in \mathbb{C}^{N_R}$ as the vector of channels from UE ℓ to relay m, the received signal at relay m is

$$\boldsymbol{r}_m = \sum_{\ell \in \mathcal{K}} \sqrt{p_\ell} \boldsymbol{h}_{\ell,m} s_\ell + e_{LI,m} + \boldsymbol{n}_{R,m}, \tag{1}$$

where $\boldsymbol{n}_{R,m} \sim \mathcal{CN}(0, \sigma_R^2 \boldsymbol{I}_{N_R})$ is the background noise, and $\boldsymbol{p} = (p_1,\ldots,p_{2K})$ is a vector of UE power allocation, while $e_{LI,m} \in \mathbb{C}^{N_R}$ models the effect of analog circuit non-ideality and the limited dynamic range of the analog-to-digital converter (ADC) at FD relay m.

The transmit power at UEs is physically limited by $P^{U,\max}$ as

$$p_k \leq P^{U,\max}, \quad k \in \mathcal{K}. \tag{2}$$

The total transmit power of UEs is bounded by $P_{\text{sum}}^{U,\max}$ to prevent their excessive interference to other networks as

$$P_{\text{sum}}^U(\boldsymbol{p}) = \sum_{k \in \mathcal{K}} p_k \leq P_{\text{sum}}^{U,\max}. \tag{3}$$

Relay m processes the received signal by applying the beamforming matrix $\boldsymbol{W}_m \in \mathcal{C}^{N_R \times N_R}$ for transmission:

$$\begin{aligned} \boldsymbol{r}_{m,b} &= \boldsymbol{W}_m \boldsymbol{r}_m \\ &= \sum_{\ell \in \mathcal{K}} \sqrt{p_\ell} \boldsymbol{W}_m \boldsymbol{h}_{\ell,m} s_\ell + \boldsymbol{W}_m (e_{LI,m} + \boldsymbol{n}_{R,m}). \end{aligned} \tag{4}$$

For simplicity it is assumed that $\boldsymbol{W}_m e_{LI,m} \sim \mathcal{CN}(0, \sigma_{SI}^2 P_m^A(\boldsymbol{p}, \boldsymbol{W}_m) I_{N_R})$ with the relay channel's instantaneous residual SI attenuation level σ_{SI}.[1] This gives

$$\mathbb{E}[||\boldsymbol{W}_m e_{LI,m}||^2] = \sigma_{SI}^2 P_m^A(\boldsymbol{p}, \boldsymbol{W}_m),$$

in calculating the transmit power at relay m by a closed-form as

$$\begin{aligned} P_m^A(\boldsymbol{p}, \boldsymbol{W}_m) &= \mathbb{E}[||\boldsymbol{r}_{m,b}||^2] \\ &= \sum_{\ell \in \mathcal{K}} p_\ell ||\boldsymbol{W}_m \boldsymbol{h}_{\ell,m}||^2 + \sigma_R^2 ||\boldsymbol{W}_m||^2 \\ &\quad + \mathbb{E}[||\boldsymbol{W}_m e_{LI,m}||^2] \\ &= \left[\sum_{\ell \in \mathcal{K}} p_\ell ||\boldsymbol{W}_m \boldsymbol{h}_{\ell,m}||^2 \right. \\ &\quad \left. + \sigma_R^2 ||\boldsymbol{W}_m||^2 \right] / (1 - \sigma_{SI}^2). \end{aligned} \tag{5}$$

[1] It is more practical to assume $e_{LI,m} \sim \mathcal{CN}(0, \bar{\sigma}_{SI}^2 P_m^A(\boldsymbol{p}, \boldsymbol{W}_m) I_{N_R})$ so $\boldsymbol{W}_m e_{LI,m} \sim \mathcal{CN}(0, \bar{\sigma}_{SI}^2 P_m^A(\boldsymbol{p}, \boldsymbol{W}_m) \boldsymbol{W}_m \boldsymbol{W}_m^H)$ resulting in $\mathbb{E}[||\boldsymbol{W}_m e_{LI,m}||^2] = \bar{\sigma}_{SI}^2 P_m^A(\boldsymbol{p}, \boldsymbol{W}_m) ||\boldsymbol{W}_m||^2$. Usually $||\boldsymbol{W}_m||^2 \leq \nu$ can be assumed so $\mathbb{E}[||\boldsymbol{W}_m e_{LI,m}||^2] = \sigma_{SI}^2 P_m^A(\boldsymbol{p}, \boldsymbol{W}_m)$ for $\sigma_{SI}^2 = \nu \bar{\sigma}_{SI}^2$

This transmit power at relay m must be physically limited by a physical parameter $P^{A,\max}$ as

$$P_m^A(\boldsymbol{p}, \boldsymbol{W}_m) \leq P^{A,\max}, m \in \mathcal{M}, \tag{6}$$

and their sum is also bounded by $P_{\text{sum}}^{R,\max}$ to control the network emission to other networks:

$$\begin{aligned} P_{\text{sum}}^R(\boldsymbol{p}, \boldsymbol{W}) &= \sum_{m\in\mathcal{M}} P_m^A(\boldsymbol{p}, \boldsymbol{W}_m) \\ &= \sum_{m\in\mathcal{M}} [\sum_{k\in\mathcal{K}} p_\ell ||\boldsymbol{W}_m \boldsymbol{h}_{\ell,m}||^2 \\ &\quad +\sigma_R^2 ||\boldsymbol{W}_m||^2]/(1-\sigma_{SI}^2) \\ &\leq P_{\text{sum}}^{R,\max}. \end{aligned} \tag{7}$$

The relays transmit the processed signals to all UEs. For the vector channel $\boldsymbol{g}_{m,k} \in \mathcal{C}^{N_R}$ from relay m to UE k and channel $\chi_{\eta,k}$ from UE $\eta \in \mathcal{U}(k)$ to UE k, the received signal at UE k is given by

$$\begin{aligned} y_k &= \sum_{m\in\mathcal{M}} \boldsymbol{g}_{m,k}^T \boldsymbol{r}_{m,b} + \sum_{\eta\in\mathcal{U}(k)} \chi_{\eta,k}\sqrt{p}_\eta \tilde{s}_\eta + n_k \\ &= \sum_{m\in\mathcal{M}} \boldsymbol{g}_{m,k}^T \left[\sum_{\ell\in\mathcal{K}} \sqrt{p_\ell}\boldsymbol{W}_m \boldsymbol{h}_{\ell,m} s_\ell + \boldsymbol{W}_m (e_{LI,m} \right. \\ &\quad \left. +\boldsymbol{n}_{R,m})\right] + \sum_{\eta\in\mathcal{U}(k)} \chi_{\eta,k}\sqrt{p}_\eta \tilde{s}_\eta + n_k, \end{aligned} \tag{8}$$

where $n_k \sim \mathcal{CN}(0, \sigma_k^2)$ is the background noise, and $|\chi_{k,k}|^2 = \sigma_{SI}^2$ as $\chi_{k,k}\tilde{s}_k$ represents the loop interference at UE k. We can rewrite (8) as

$$\begin{aligned} y_k &= \sqrt{p_{a(k)}} \sum_{m\in\mathcal{M}} \boldsymbol{g}_{m,k}^T \boldsymbol{W}_m \boldsymbol{h}_{a(k),m} s_{a(k)} \\ &\quad +\sqrt{p_k} \sum_{m\in\mathcal{M}} \boldsymbol{g}_{m,k}^T \boldsymbol{W}_m \boldsymbol{h}_{k,m} s_k \\ &\quad + \sum_{m\in\mathcal{M}} \boldsymbol{g}_{m,k}^T \left[\sum_{\ell\in\mathcal{K}\setminus\{k,a(k)\}} \sqrt{p_\ell}\boldsymbol{W}_m \boldsymbol{h}_{\ell,m} s_\ell \right. \\ &\quad \left. +\boldsymbol{W}_m (e_{LI,m} + \boldsymbol{n}_{R,m})\right] \\ &\quad + \sum_{\eta\in\mathcal{U}(k)} \chi_{\eta,k}\sqrt{p}_\eta \tilde{s}_\eta + n_k. \end{aligned} \tag{9}$$

Note that the first term in (9) is the desired signal component, the third term is the inter-pair interference and the last two terms are noise. UE k can cancel the self-interference by the second term using the channel state information of the forward channels $\mathbf{h}_{k,m}$ from itself to the relays and backward channels $\mathbf{g}_{m,k}$ from the relays to itself as well as the beamforming matrix $\mathbf{W}_m$. The challenges here is that the loop SI term $\sum_{\eta\in\mathcal{U}(k)} \chi_{\eta,k}\sqrt{p}_\eta \tilde{s}_\eta$, which may be strong due to the proximity of UEs in $\mathcal{U}(k)$, cannot be nulled out. This means more power should be given to the relays but it leads to more FD SI at the relays.

Furthermore, for $\boldsymbol{f}_{m,k}^H \triangleq \boldsymbol{g}_{m,k}^T$, the signal-to-interference-plus-noise ratio (SINR) at UE k' receiver can be calculated as

$$\begin{aligned} \gamma_k(\boldsymbol{p}, \boldsymbol{W}) &= p_{a(k)} \left| \sum_{m\in\mathcal{M}} \boldsymbol{f}_{m,k}^H \boldsymbol{W}_m \boldsymbol{h}_{a(k),m} \right|^2 \\ &\quad / \left[\sum_{\ell\in\mathcal{K}\setminus\{k,a(k)\}} p_\ell \left| \sum_{m\in\mathcal{M}} \boldsymbol{f}_{m,k}^H \boldsymbol{W}_m \boldsymbol{h}_{\ell,m} \right|^2 \right. \\ &\quad \left. +\sigma_R^2 \sum_{m\in\mathcal{M}} ||\boldsymbol{f}_{m,k}^H \boldsymbol{W}_m||^2 \right. \\ &\quad +\frac{\sigma_{SI}^2}{1-\sigma_{SI}^2} \sum_{m\in\mathcal{M}} ||\boldsymbol{g}_{m,k}||^2 \left(\sum_{\ell\in\mathcal{K}} p_\ell ||\boldsymbol{W}_m \boldsymbol{h}_{\ell,m}||^2 \right. \\ &\quad \left. \left. +\sigma_R^2 ||\boldsymbol{W}_m||^2 \right) + \sum_{\eta\in\mathcal{U}(k)} |\chi_{\eta,k}|^2 p_\eta + \sigma_k^2 \right]. \end{aligned} \tag{10}$$

Under the definitions

$$\begin{aligned} \mathcal{L}_{k,\ell}(\boldsymbol{W}) &\triangleq \sum_{m\in\mathcal{M}} \boldsymbol{f}_{m,k}^H \boldsymbol{W}_m \boldsymbol{h}_{\ell,m}, \\ \mathcal{L}_k(\boldsymbol{W}) &\triangleq \left[\boldsymbol{f}_{1,k}^H \boldsymbol{W}_1 \quad \boldsymbol{f}_{2,k}^H \boldsymbol{W}_2 \quad \ldots \quad \boldsymbol{f}_{M,k}^H \boldsymbol{W}_M\right], \end{aligned} \tag{11}$$

it follows that

$$\begin{aligned} \gamma_k(\boldsymbol{p}, \boldsymbol{W}) &= p_{a(k)} |\mathcal{L}_{k,a(k)}(\boldsymbol{W})|^2 \\ &\quad / \left[\sum_{\substack{\ell\in\mathcal{K}\setminus \\ \{k,a(k)\}}} p_\ell |\mathcal{L}_{k,\ell}(\boldsymbol{W})|^2 + \sigma_R^2 ||\mathcal{L}_k(\boldsymbol{W})||^2 \right. \\ &\quad +\frac{\sigma_{SI}^2}{1-\sigma_{SI}^2} \sum_{m\in\mathcal{M}} ||\boldsymbol{g}_{m,k}||^2 \left(\sum_{\ell\in\mathcal{K}} p_\ell ||\boldsymbol{W}_m \boldsymbol{h}_{\ell,m}||^2 \right. \\ &\quad \left. \left. +\sigma_R^2 ||\boldsymbol{W}_m||^2 \right) + \sum_{\eta\in\mathcal{U}(k)} |\chi_{\eta,k}|^2 p_\eta + \sigma_k^2 \right]. \end{aligned} \tag{12}$$

In FD TWR, the performance of interest is the exchange information throughput of UE pairs:

$$\begin{aligned} R_k(\boldsymbol{p}, \boldsymbol{W}) &= \ln(1+\gamma_k(\boldsymbol{p}, \boldsymbol{W})) + \ln(1+\gamma_{a(k)}(\boldsymbol{p}, \boldsymbol{W})), \\ &\quad k = 1, \ldots, K. \end{aligned} \tag{13}$$

The problem of maximin exchange information throughput optimization subject to transmit power constraints is then formulated as

$$\max_{\boldsymbol{W}, \boldsymbol{p}} \quad \min_{k=1,\ldots,K} [\ln(1+\gamma_k(\boldsymbol{p}, \boldsymbol{W})) + \ln(1+\gamma_{a(k)}(\boldsymbol{p}, \boldsymbol{W}))] \tag{14a}$$

$$\text{s.t.} \quad (2), (3), (6), (7). \tag{14b}$$

Another problem, which attracted recent attention in 5G [23], [24] is the following problem of maximizing the network energy-efficiency (EE) subject to UE QoS in terms of the exchange information throughput thresholds:

$$\max_{\boldsymbol{W}, \boldsymbol{p}} \quad \sum_{k=1}^K \left[\ln(1+\gamma_k(\boldsymbol{p}, \boldsymbol{W})) + \ln(1+\gamma_{a(k)}(\boldsymbol{p}, \boldsymbol{W}))\right] / [\zeta(P_{\text{sum}}^U(\mathbf{p}) + P_{\text{sum}}^R(\mathbf{p}, \mathbf{W})) + MP^{\text{R}} + 2KP^{\text{U}}] \tag{15a}$$

$$\text{s.t.} \quad (2), (3), (6), (7), \tag{15b}$$

$$R_k(\boldsymbol{p}, \boldsymbol{W}) \geq r_k, k = 1, \ldots, K, \tag{15c}$$

where ζ, P^{R} and P^{U} are the reciprocal of drain efficiency of power amplifier, the circuit powers of the relay and UE, respectively, and r_k sets the exchange throughput threshold for UE pairs.

The next two subsections are devoted to computational solution for problems (14) and (15), respectively.

A. FD TWR maximin exchange information throughput optimization

By introducing new nonnegative variables

$$\beta_k = 1/p_k^2 > 0, k \in \mathcal{K}, \tag{16}$$

and functions

$$\begin{gathered}\Psi_{k,\ell}(\boldsymbol{W},\alpha,\beta) \triangleq |\mathcal{L}_{k,\ell}(\boldsymbol{W})|^2/\sqrt{\alpha\beta}, (k,\ell) \in \mathcal{K}\times\mathcal{K},\\ \Upsilon_k(\boldsymbol{W},\alpha) \triangleq ||\mathcal{L}_k(\boldsymbol{W})||^2/\sqrt{\alpha}, k \in \mathcal{K},\\ \Phi_{\ell,m}(\boldsymbol{W}_m,\alpha,\beta) \triangleq ||\boldsymbol{h}_{\ell,m}^H\boldsymbol{W}_m||^2/\sqrt{\alpha\beta}, \quad (\ell,m) \in \mathcal{K}\times\mathcal{M},\end{gathered} \tag{17}$$

which are convex [25], (12) can be re-expressed by

$$\begin{aligned}\gamma_k(\boldsymbol{p},\boldsymbol{W}) &= |\mathcal{L}_{k,a(k)}(\boldsymbol{W})|^2/\sqrt{\beta_{a(k)}}\\ &\times\left[\sum_{\ell\in\mathcal{K}\setminus\{k,a(k)\}}\Psi_{k,\ell}(\boldsymbol{W},1,\beta_\ell) + \sigma_R^2\Upsilon_k(\boldsymbol{W},1)\right.\\ &+\frac{\sigma_{SI}^2}{1-\sigma_{SI}^2}\sum_{m\in\mathcal{M}}||\boldsymbol{g}_{m,k}||^2(\sum_{\ell\in\mathcal{K}}\Phi_{\ell,m}(\boldsymbol{W}_m,1,\beta_\ell)\\ &\left.+\sigma_R^2\langle\boldsymbol{W}_m^H\boldsymbol{W}_m\rangle) + \sum_{\eta\in\mathcal{U}(k)}|\chi_{\eta,k}|^2/\sqrt{\beta_\eta} + \sigma_k^2\right].\end{aligned} \tag{18}$$

Similarly to [26] and [13, Th. 1] we can prove the following result.

Theorem 1: The optimization problem (14), which is maximization of nonconcave objective function over a nonconvex set, can be equivalently rewritten as the following problem of maximizing a nonconcave objective function over a set of convex constraints:

$$\begin{aligned}\max_{\boldsymbol{W},\boldsymbol{\alpha},\boldsymbol{\beta}}\quad & f(\boldsymbol{W},\boldsymbol{\alpha},\boldsymbol{\beta}) \triangleq\\ & \min_{k=1,\ldots,K}\left[\ln(1+|\mathcal{L}_{k,a(k)}(\boldsymbol{W})|^2/\sqrt{\alpha_k\beta_{a(k)}})\right.\\ & \left.+\ln(1+|\mathcal{L}_{a(k),k}(\boldsymbol{W})|^2/\sqrt{\alpha_{a(k)}\beta_k})\right] && \text{(19a)}\\ \text{s.t.}\quad & \sum_{\ell\in\mathcal{K}\setminus\{k,a(k)\}}\Psi_{k,\ell}(\boldsymbol{W},\alpha_k,\beta_\ell) + \sigma_R^2\Upsilon_k(\boldsymbol{W},\alpha_k)\\ & +\sum_{\eta\in\mathcal{U}(k)}|\chi_{\eta,k}|^2/\sqrt{\alpha_k\beta_\eta}\\ & +\frac{\sigma_{SI}^2}{1-\sigma_{SI}^2}\sum_{m\in\mathcal{M}}||\boldsymbol{g}_{m,k}||^2(\sum_{\ell\in\mathcal{K}}\Phi_{\ell,m}(\boldsymbol{W}_m,\alpha_k,\beta_\ell)\\ & +\sigma_R^2||\boldsymbol{W}_m||^2/\sqrt{\alpha_k}) + \sigma_k^2/\sqrt{\alpha_k} \le 1, && \text{(19b)}\\ & \beta_k \ge 1/(P^{U,\max})^2, k\in\mathcal{K}, && \text{(19c)}\\ & P_{\mathrm{sum}}^U(\boldsymbol{\beta}) := \sum_{k\in\mathcal{K}}1/\sqrt{\beta_k} \le P_{\mathrm{sum}}^{U,\max}, && \text{(19d)}\\ & \sum_{\ell\in\mathcal{K}}\Phi_{\ell,m}(\boldsymbol{W}_m,1,\beta_\ell) + \sigma_R^2||\boldsymbol{W}_m||^2\\ & \le (1-\sigma_{SI}^2)P_m^{A,\max}, m\in\mathcal{M}, && \text{(19e)}\\ & \sum_{m\in\mathcal{M}}\left[\sum_{\ell\in\mathcal{K}}\Phi_{\ell,m}(\boldsymbol{W}_m,1,\beta_\ell) + \sigma_R^2||\boldsymbol{W}_m||^2\right]\\ & \le (1-\sigma_{SI}^2)P_{\mathrm{sum}}^{R,\max}. && \text{(19f)}\end{aligned}$$

As in [13] the main issue is to handle the nonconcave objective function in (19a). Indeed, one can use [13, Th. 2] for lower bounding the objective function in (19a) by a concave function, which is a reciprocal of a positive linear functions over a complex trust region involving all concerned variables. By the following theorem we provide a new and better lower bound under a simpler trust region involving only the beamforming matrix $\mathbf{W}$, which results in expanded local search areas, accelerating convergence of the designed algorithm. This is a one-step approximation that is in contrast to the multi-step approximation in [13].

Theorem 2: At any $(\boldsymbol{W}^{(\kappa)},\boldsymbol{\alpha}^{(\kappa)},\boldsymbol{\beta}^{(\kappa)})$ feasible for the convex constraints (19b)-(19f), it is true that

$$\begin{aligned}\ln(1+|\mathcal{L}_{k,a(k)}(\boldsymbol{W})|^2/\sqrt{\alpha_k\beta_{a(k)}}) \quad &\ge\\ f_{k,a(k)}^{(\kappa)}(\boldsymbol{W},\alpha_k,\beta_{a(k)})\end{aligned} \tag{20}$$

over the trust region

$$\begin{aligned}2\Re\{\mathcal{L}_{k,a(k)}(\boldsymbol{W})(\mathcal{L}_{k,a(k)}(\boldsymbol{W}^{(\kappa)}))^*\}\\ -|\mathcal{L}_{k,a(k)}(\boldsymbol{W}^{(\kappa)})|^2 \quad > \quad 0,\end{aligned} \tag{21}$$

for

$$\begin{aligned}f_{k,a(k)}^{(\kappa)}(\boldsymbol{W},\alpha_k,\beta_{a(k)}) \quad &=\\ \ln(1+x_{k,a(k)}^{(\kappa)}) + a_{k,a(k)}^{(\kappa)}\,[2-&\\ \frac{|\mathcal{L}_{k,a(k)}(\boldsymbol{W}^{(\kappa)})|^2}{2\Re\{\mathcal{L}_{k,a(k)}(\boldsymbol{W})(\mathcal{L}_{k,a(k)}(\boldsymbol{W}^{(\kappa)}))^*\} - |\mathcal{L}_{k,a(k)}(\boldsymbol{W}^{(\kappa)})|^2}&\\ -\sqrt{\alpha_k\beta_{a(k)}}/\sqrt{\alpha_k^{(\kappa)}\beta_{a(k)}^{(\kappa)}}\Big]&\end{aligned} \tag{22}$$

with $x_{k,a(k)}^{(\kappa)} \triangleq |\mathcal{L}_{k,a(k)}(\boldsymbol{W}^{(\kappa)})|^2/\sqrt{\alpha_k^{(\kappa)}\beta_{a(k)}^{(\kappa)}}$ and $a_{k,a(k)}^{(\kappa)} \triangleq x_{k,a(k)}^{(\kappa)})/(x_{k,a(k)}^{(\kappa)}+1) > 0$.

Proof: (22) follows by applying inequality (59) in the Appendix for

$$x = 1/|\mathcal{L}_{k,a(k)}(\boldsymbol{W})|^2, y = \sqrt{\alpha_k\beta_{a(k)}}$$

and

$$\bar{x} = 1/|\mathcal{L}_{k,a(k)}(\boldsymbol{W}^{(\kappa)})|^2, \bar{y} = \sqrt{\alpha_k^{(\kappa)}\beta_{a(k)}^{(\kappa)}}$$

and then the inequality

$$\begin{aligned}1/|\mathcal{L}_{k,a(k)}(\boldsymbol{W})|^2 \quad &\le \quad 1/\Big(2\Re\{\mathcal{L}_{k,a(k)}(\boldsymbol{W})(\mathcal{L}_{k,a(k)}(\boldsymbol{W}^{(\kappa)}))^*\}\\ &\qquad -|\mathcal{L}_{k,a(k)}(\boldsymbol{W}^{(\kappa)})|^2\Big)\end{aligned} \tag{23}$$

over the trust region (21). □

By Algorithm 1 we propose a path-following procedure for computing (19), which solves the following convex optimization problem of inner approximation at the κth iteration to

generate the next feasible point $(\boldsymbol{W}^{(\kappa+1)}, \boldsymbol{\alpha}^{(\kappa+1)}, \boldsymbol{\beta}^{(\kappa+1)})$:

$$\begin{aligned} \max_{\boldsymbol{W},\boldsymbol{\alpha},\boldsymbol{\beta}} \quad & \min_{k=1,\ldots,K} [f_{k,a(k)}^{(\kappa)}(\boldsymbol{W}, \alpha_k, \beta_{a(k)}) \\ & \qquad + f_{a(k),k}^{(\kappa)}(\boldsymbol{W}, \alpha_{a(k)}, \beta_k)] \\ \text{s.t.} \quad & (19b) - (19f), (21). \end{aligned} \tag{24}$$

Similarly to [13, Alg. 1], it can be shown that the sequence $\{(\boldsymbol{W}^{(\kappa)}, \boldsymbol{\alpha}^{(\kappa)}, \boldsymbol{\beta}^{(\kappa)})\}$ generated by Algorithm 1 at least converges to a local optimal solution of (19).[2]

Algorithm 1 Path-following algorithm for FD TWR exchange throughput optimization

initialization: Set $\kappa = 0$. Initialize a feasible point $(\boldsymbol{W}^{(0)}, \boldsymbol{\alpha}^{(0)}, \boldsymbol{\beta}^{(0)})$ for the convex constraints (19b)-(19f) and $R_1 = f(\boldsymbol{W}^{(0)}, \boldsymbol{\alpha}^{(0)}, \boldsymbol{\beta}^{(0)})$.

repeat

- $R_0 = R_1$.
- Solve the convex optimization problem (24) to obtain the solution $(\boldsymbol{W}^{(\kappa+1)}, \boldsymbol{\alpha}^{(\kappa+1)}, \boldsymbol{\beta}^{(\kappa+1)})$.
- Update $R_1 = f(\boldsymbol{W}^{(\kappa+1)}, \boldsymbol{\alpha}^{(\kappa+1)}, \boldsymbol{\beta}^{(\kappa+1)})$.
- Reset $\kappa \to \kappa + 1$.

until $\frac{R_1 - R_0}{R_0} \leq \epsilon$ for given tolerance $\epsilon > 0$.

B. FD TWR energy-efficiency maximization

We return to consider the optimization problem (15), which can be shown similarly to Theorem 1 to be equivalent to the following optimization problem under the variable change (16):

$$\max_{\boldsymbol{W},\boldsymbol{\alpha},\boldsymbol{\beta}} \; F(\boldsymbol{W}, \boldsymbol{\alpha}, \boldsymbol{\beta}) \quad \text{s.t.} \quad (19b) - (19f), \tag{25a}$$

$$\tilde{R}_k(\mathbf{W}, \boldsymbol{\alpha}, \boldsymbol{\beta}) \geq r_k, k = 1, \ldots, K, \tag{25b}$$

for

$$\begin{aligned} F(\boldsymbol{W}, \boldsymbol{\alpha}, \boldsymbol{\beta}) &\triangleq \left[\sum_{k=1}^{K} \tilde{R}_k(\mathbf{W}, \boldsymbol{\alpha}, \boldsymbol{\beta})\right] / \pi(\boldsymbol{\beta}, \boldsymbol{W}), \\ \tilde{R}_k(\mathbf{W}, \boldsymbol{\alpha}, \boldsymbol{\beta}) &\triangleq \ln\left(1 + |\mathcal{L}_{k,a(k)}(\boldsymbol{W})|^2 / \sqrt{\alpha_k \beta_{a(k)}}\right) \\ &\quad + \ln\left(1 + |\mathcal{L}_{a(k),k}(\boldsymbol{W})|^2 / \sqrt{\alpha_{a(k)} \beta_k}\right), \end{aligned}$$

and

$$\begin{aligned} \pi(\boldsymbol{\beta}, \boldsymbol{W}) \triangleq & \sum_{k \in \mathcal{K}} \zeta / \sqrt{\beta_k} + (\zeta / (1 - \sigma_{SI}^2)) \\ & \times \sum_{m \in \mathcal{M}} \left[\sum_{\ell \in \mathcal{K}} \Phi_{\ell,m}(\boldsymbol{W}_m, 1, \beta_\ell) \right. \\ & \left. + \sigma_R^2 ||\boldsymbol{W}_m||^2\right] + MP^{\mathrm{R}} + 2KP^{\mathrm{U}}. \end{aligned} \tag{26}$$

The objective function in (25a) is nonconcave and constraint (25b) is nonconvex.

Suppose that $(\boldsymbol{W}^{(\kappa)}, \boldsymbol{\alpha}^{(\kappa)}, \boldsymbol{\beta}^{(\kappa)})$ is a feasible point for (25) found from the $(\kappa - 1)$th iteration. Applying inequality (58) in the Appendix for

$$x = 1/|\mathcal{L}_{k,a(k)}(\boldsymbol{W})|^2, y = \sqrt{\alpha_k \beta_{a(k)}}, t = \pi(\boldsymbol{\beta}, \boldsymbol{W})$$

and

$$\bar{x} = 1/|\mathcal{L}_{k,a(k)}(\boldsymbol{W}^{(\kappa)})|^2, \bar{y} = \sqrt{\alpha_k^{(\kappa)} \beta_{a(k)}^{(\kappa)}}, \bar{t} = \pi(\boldsymbol{\beta}^{(\kappa)}, \boldsymbol{W}^{(\kappa)})$$

and using inequality (23) yield the following new and tighter bound compared to [13, (36)] for the terms of the objective function in (25a), which involves only one approximation step:

$$\begin{aligned} \left[\ln(1 + |\mathcal{L}_{k,a(k)}(\boldsymbol{W})|^2 / \sqrt{\alpha_k \beta_{a(k)}})\right] / \pi(\boldsymbol{\beta}, \boldsymbol{W}) \quad \geq \\ F_{k,a(k)}^{(\kappa)}(\boldsymbol{W}, \alpha_k, \boldsymbol{\beta}) \end{aligned} \tag{27}$$

over the trust region (21), where

$$\begin{aligned} F_{k,a(k)}^{(\kappa)}(\boldsymbol{W}, \alpha_k, \boldsymbol{\beta}) \triangleq \\ p_{k,a(k)}^{(\kappa)} + q_{k,a(k)}^{(\kappa)} [2 - \\ \frac{|\mathcal{L}_{k,a(k)}(\boldsymbol{W}^{(\kappa)})|^2}{2\Re\{\mathcal{L}_{k,a(k)}(\boldsymbol{W})(\mathcal{L}_{k,a(k)}(\boldsymbol{W}^{(\kappa)}))^*\} - |\mathcal{L}_{k,a(k)}(\boldsymbol{W}^{(\kappa)})|^2} \\ - \sqrt{\alpha_k \beta_{a(k)}} / \sqrt{\alpha_k^{(\kappa)} \beta_{a(k)}^{(\kappa)}}] - r_{k,a(k)}^{(\kappa)} \pi(\boldsymbol{\beta}, \boldsymbol{W}), \end{aligned}$$

and

$$\begin{aligned} x_{k,a(k)}^{(\kappa)} &= |\mathcal{L}_{k,a(k)}(\boldsymbol{W}^{(\kappa)})|^2 / \sqrt{\alpha_k^{(\kappa)} \beta_{a(k)}^{(\kappa)}}, \\ t^{(\kappa)} &= \pi(\boldsymbol{\beta}^{(\kappa)}, \boldsymbol{W}^{(\kappa)}), \\ p_{k,a(k)}^{(\kappa)} &= 2\left[\ln(1 + x_{k,a(k)}^{(\kappa)})\right] / t^{(\kappa)} > 0, \\ q_{k,a(k)}^{(\kappa)} &= x_{k,a(k)}^{(\kappa)} / ((x_{k,a(k)}^{(\kappa)} + 1) t^{(\kappa)}) > 0, \\ r_{k,a(k)}^{(\kappa)} &= \left[\ln(1 + x_{k,a(k)}^{(\kappa)})\right] / (t^{(\kappa)})^2 > 0. \end{aligned} \tag{28}$$

Furthermore, we use $f_{k,a(k)}^{(\kappa)}$ defined from (20) to provide the following inner convex approximation for the nonconvex constraint (25b):

$$f_{k,a(k)}^{(\kappa)}(\boldsymbol{W}, \alpha_k, \beta_{a(k)}) + f_{a(k),k}^{(\kappa)}(\boldsymbol{W}, \alpha_{a(k)}, \beta_k) \geq r_k. \tag{29}$$

By Algorithm 2 we propose a path-following procedure for computing (25), which solves the following convex optimization problem at the κth iteration to generate the next feasible point $(\boldsymbol{W}^{(\kappa+1)}, \boldsymbol{\alpha}^{(\kappa+1)}, \boldsymbol{\beta}^{(\kappa+1)})$:

$$\begin{aligned} \max_{\boldsymbol{W},\boldsymbol{\alpha},\boldsymbol{\beta}} \quad & F^{(\kappa)}(\boldsymbol{W}, \boldsymbol{\alpha}, \boldsymbol{\beta}) \triangleq \sum_{k=1}^{K} [F_{k,a(k)}^{(\kappa)}(\boldsymbol{W}, \alpha_k, \boldsymbol{\beta}) \\ & \qquad + F_{a(k),k}^{(\kappa)}(\boldsymbol{W}, \alpha_{a(k)}, \boldsymbol{\beta})] \qquad (30a) \\ \text{s.t.} \quad & (19b) - (19f), (21), (29) \qquad (30b) \end{aligned}$$

Analogously to Algorithm 1, the sequence $\{(\boldsymbol{W}^{(\kappa)}, \boldsymbol{\alpha}^{(\kappa)}, \boldsymbol{\beta}^{(\kappa)})\}$ generated by Algorithm 2 at least converges to a local optimal solution of (25).

An initial feasible point $(\boldsymbol{W}^{(0)}, \boldsymbol{\alpha}^{(0)}, \boldsymbol{\beta}^{(0)})$ for initializing Algorithm 2 can be found by using Algorithm 1 for computing (14), which terminates upon

$$\min_{k=1,\ldots,K} R_k(\boldsymbol{W}^{(\kappa)}, \boldsymbol{\alpha}^{(\kappa)}, \boldsymbol{\beta}^{(\kappa)}) / r_k \geq 1 \tag{31}$$

to satisfy (25b).

[2] As mentioned in [27, Remark] this desired property of a limit point indeed does not require the differentiability of the objective function

Algorithm 2 Path-following algorithm for FD TWR energy-efficiency

initialization: Set $\kappa = 0$. Initialize a feasible point $(\boldsymbol{W}^{(0)}, \boldsymbol{\alpha}^{(0)}, \boldsymbol{\beta}^{(0)})$ for (25) and $e_1 = F(\boldsymbol{W}^{(0)}, \boldsymbol{\alpha}^{(0)}, \boldsymbol{\beta}^{(0)})$.

repeat

- $e_0 = e_1$.
- Solve the convex optimization problem (30) to obtain the solution $(\boldsymbol{W}^{(\kappa+1)}, \boldsymbol{\alpha}^{(\kappa+1)}, \boldsymbol{\beta}^{(\kappa+1)})$.
- Update $e_1 = F(\boldsymbol{W}^{(\kappa+1)}, \boldsymbol{\alpha}^{(\kappa+1)}, \boldsymbol{\beta}^{(\kappa+1)})$.
- Reset $\kappa \to \kappa + 1$.

until $\frac{e_1 - e_0}{e_0} \leq \epsilon$ for given tolerance $\epsilon > 0$.

III. Time-fraction-wise HD two-way relaying

Through the FD-based TWR detailed in the previous section one can see the following obvious issues for its practical implementations:

- It is difficult to attenuate FD SI at the UEs and relays to a level that realizes the benefits by FD. The FD SI is even more severe at the relays, which are equipped with multiple antennas;
- Inter-FD-user interference cannot be controlled;
- It is technically difficult to implement FD at UEs, which particularly requires two antennas per UE.

We now propose a new way for UE information exchange via HD TWR within the time slot as illustrated by Fig. 2, where at time-fraction $0 < \tau < 1$ all UEs send information to the relays and at the remaining time fraction $(1 - \tau)$ the relays send the beamformed signals to UEs. This alternative has the following advantages:

- Each relay uses all available $2N_R$ antennas for separated receiving and transmitting signals;
- UEs need only a single antenna to implement the conventional HD, which transmits signal and receive signals in separated time fractions.

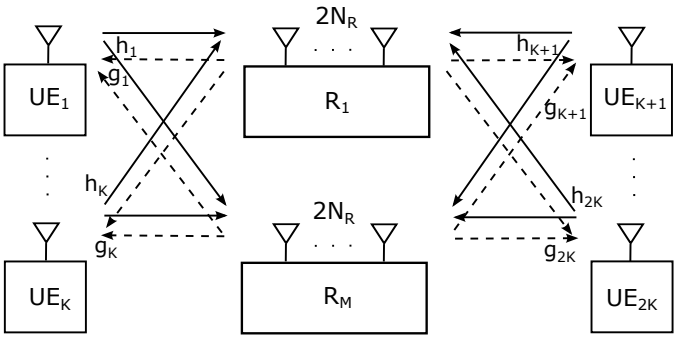

Fig. 2. Two-way relay networks with multiple single-antenna users and multiple multi-antenna relays.

Suppose that UE k uses the power τp_k to send information to the relay. The following physical limitation is imposed:

$$p_k \leq \bar{P}_{\mathrm{UE}}, k \in \mathcal{K}, \tag{32}$$

where $\bar{P}_{\mathrm{UE}}$ is a physical parameter to signify the hardware limit in transmission during time-fractions. Typically, $\bar{P}_{\mathrm{UE}} = 3P^{U,\max}$ for $P^{U,\max}$ defined from (2).

As in (3), the power budget of all UEs is $P_{\mathrm{sum}}^{U,\max}$:

$$P_{\mathrm{sum}}^{U}(\boldsymbol{p}) = \tau \sum_{k \in \mathcal{K}} p_k \leq P_{\mathrm{sum}}^{U,\max}. \tag{33}$$

The received signal at relay m can be simply written as

$$\boldsymbol{r}_m = \sum_{\ell \in \mathcal{K}} \sqrt{\tau p_\ell} \boldsymbol{h}_{\ell,m} s_\ell + \boldsymbol{n}_{R,m}^{(\tau)}, \tag{34}$$

where $\mathbf{n}_{R,m}^{(\tau)} \in \mathcal{CN}(0, \tau\sigma_R^2 \mathbf{I}_{2N_R})$ and $\boldsymbol{h}_{\ell,m} \in \mathbb{C}^{2N_R}$ is the vector of channels from UE ℓ to relay m.

Relay m processes the received signal by applying the beamforming matrix $\mathbf{W}_m \in \mathbb{C}^{2N_R \times 2N_R}$ for transmission:

$$\boldsymbol{r}_{m,b} = \boldsymbol{W}_m \boldsymbol{r}_m = \sum_{\ell \in \mathcal{K}} \sqrt{\tau p_\ell} \boldsymbol{W}_m \boldsymbol{h}_{\ell,m} s_\ell + \boldsymbol{W}_m \boldsymbol{n}_{R,m}^{(\tau)}. \tag{35}$$

Given the physical parameter $P^{A,\max}$ as in (6) and then $\bar{P}_R = 3P^{A,\max}$, the transmit power at relay m is physically limited as

$$\begin{aligned} P_m^A(\boldsymbol{p}, \boldsymbol{W}_m, \tau) &= \tau \left[\sum_{\ell \in \mathcal{K}} p_\ell ||\boldsymbol{W}_m \boldsymbol{h}_{\ell,m}||^2 + \sigma_R^2 ||\boldsymbol{W}_m||^2 \right] \\ &\leq \bar{P}_R, \quad m \in \mathcal{M}. \end{aligned} \tag{36}$$

Given a budget $P_{\mathrm{sum}}^{R,\max}$ as in (7), the sum transmit power by the relays is also constrained as

$$\begin{aligned} P_{\mathrm{sum}}^{R}(\tau, \boldsymbol{p}, \boldsymbol{W}) &= (1-\tau) \sum_{m \in \mathcal{M}} P_m^A(\boldsymbol{p}, \boldsymbol{W}_m, \tau) \\ &= (1-\tau)\tau \sum_{m \in \mathcal{M}} \left(\sum_{\ell \in \mathcal{K}} p_\ell ||\boldsymbol{W}_m \boldsymbol{h}_{\ell,m}||^2 \right. \\ &\quad \left. + \sigma_R^2 ||\boldsymbol{W}_m||^2 \right) \\ &\leq P_{\mathrm{sum}}^{R,\max}. \end{aligned} \tag{37}$$

The received signal at UE k is virtually expressed as

$$\begin{aligned} y_k &= \sqrt{\tau p_{a(k)}} \sum_{m \in \mathcal{M}} \boldsymbol{g}_{m,k}^T \boldsymbol{W}_m \boldsymbol{h}_{a(k),m} s_{a(k)} \\ &\quad + \sqrt{\tau p_k} \sum_{m \in \mathcal{M}} \boldsymbol{g}_{m,k}^T \boldsymbol{W}_m \boldsymbol{h}_{k,m} s_k \\ &\quad + \sum_{m \in \mathcal{M}} \boldsymbol{g}_{m,k}^T \left(\sum_{\ell \in \mathcal{K} \setminus \{k, a(k)\}} \sqrt{\tau p_\ell} \boldsymbol{W}_m \boldsymbol{h}_{\ell,m} s_\ell \right. \\ &\quad \left. + \boldsymbol{W}_m \boldsymbol{n}_{R,m}^{(\tau)} \right) + n_k. \end{aligned} \tag{38}$$

Under the definitions

$$\begin{aligned} \mathcal{L}_{k,\ell}(\boldsymbol{W}) &= \sum_{m \in \mathcal{M}} \boldsymbol{f}_{m,k}^H \boldsymbol{W}_m \boldsymbol{h}_{\ell,m}, \\ \mathcal{L}_k(\boldsymbol{W}) &= \left[\boldsymbol{f}_{1,k}^H \boldsymbol{W}_1 \quad \boldsymbol{f}_{2,k}^H \boldsymbol{W}_2 \quad \ldots \quad \boldsymbol{f}_{M,k}^H \boldsymbol{W}_M \right], \end{aligned} \tag{39}$$

the SINR at UE k can be calculated as

$$\begin{aligned} \gamma_k(\boldsymbol{p}, \boldsymbol{W}, \tau) &= \\ p_{a(k)} |\mathcal{L}_{k,a(k)}(\boldsymbol{W})|^2 / &\left[\sum_{\ell \in \mathcal{K} \setminus \{k, a(k)\}} p_\ell |\mathcal{L}_{k,\ell}(\boldsymbol{W})|^2 \right. \\ &\left. + \sigma_R^2 ||\mathcal{L}_k(\boldsymbol{W})||^2 + \sigma_k^2/\tau \right]. \end{aligned} \tag{40}$$

Thus, the throughput at the kth UE pair is defined by the following function of beamforming matrix $\boldsymbol{W} = \{\boldsymbol{W}_m\}_{m\in\mathcal{M}}$, power allocation vector $\boldsymbol{p}$ and time-fraction τ:

$$\begin{aligned} R_k(\tau,\boldsymbol{p},\boldsymbol{W}) &= (1-\tau)\ln(1+\gamma_k(\boldsymbol{p},\boldsymbol{W},\tau)) \\ &\quad +(1-\tau)\ln(1+\gamma_{a(k)}(\boldsymbol{p},\boldsymbol{W},\tau)), \\ &\quad k=1,\ldots,K. \end{aligned} \tag{41}$$

Similarly to (14), the problem of maximin exchange information throughput optimization subject to transmit power constraints is formulated as

$$\max_{0<\tau<1,\boldsymbol{W},\boldsymbol{p}} \quad \min_{k=1,\ldots,K}(1-\tau)\left[\ln(1+\gamma_k(\boldsymbol{p},\boldsymbol{W},\tau)) + \ln(1+\gamma_{a(k)}(\boldsymbol{p},\boldsymbol{W},\tau))\right] \tag{42a}$$

$$\text{s.t.} \qquad (32),(33),(36),(37), \tag{42b}$$

while the problem of maximizing the network EE subject to UE QoS in terms of the exchange information throughput thresholds is formulated similarly to (15) as

$$\max_{0<\tau<1,\boldsymbol{W},\boldsymbol{p}} \quad \sum_{k=1}^{K}(1-\tau)\left[\ln(1+\gamma_k(\boldsymbol{p},\boldsymbol{W},\tau)) + \ln(1+\gamma_{a(k)}(\boldsymbol{p},\boldsymbol{W},\tau))\right]/[\zeta(P^U_{\rm sum}(\tau,\mathbf{p}) + P^R_{\rm sum}(\tau,\mathbf{p},\mathbf{W})) + MP^{\rm R} + 2KP^{\rm U}] \tag{43a}$$

$$\text{s.t.} \qquad (32),(33),(36),(37) \tag{43b}$$

$$R_k(\tau,\boldsymbol{p},\boldsymbol{W}) \geq r_k, k=1,\cdots,K. \tag{43c}$$

The next two subsections are devoted to their computation.

A. TF-wise HD TWR maximin exchange information throughput optimization

Similarly to (19), problem (42) of maximin exchange information throughput optimization is equivalently expressed by the following optimization problem with using new variables $\boldsymbol{\beta} = (\beta_1,\ldots,\beta_{2K})^T$ defined from (16):

$$\max_{0<\tau<1,\boldsymbol{W},\atop \boldsymbol{\alpha},\boldsymbol{\beta}} \quad \min_{k=1,\ldots,K}(1-\tau) \times \left[\ln(1+|\mathcal{L}_{k,a(k)}(\boldsymbol{W})|^2/\sqrt{\alpha_k\beta_{a(k)}}) + \ln(1+|\mathcal{L}_{a(k),k}(\boldsymbol{W})|^2/\sqrt{\alpha_{a(k)}\beta_k})\right] \tag{44a}$$

$$\text{s.t.} \quad \sum_{\ell\in\mathcal{K}\setminus\{k,a(k)\}} \Psi_{k,\ell}(\boldsymbol{W},\alpha_k,\beta_\ell) + \sigma_R^2\Upsilon_k(\boldsymbol{W},\alpha_k) + \sigma_k^2/\tau\sqrt{\alpha_k} \leq 1, k\in\mathcal{K}, \tag{44b}$$

$$\beta_k \geq 1/(\bar{P}_{\rm UE})^2,\ k\in\mathcal{K}, \tag{44c}$$

$$\sum_{k\in\mathcal{K}} \tau/\sqrt{\beta_k} \leq P^{U,\max}_{\rm sum}, \tag{44d}$$

$$\tau[\sum_{\ell\in\mathcal{K}} \Phi_{\ell,m}(\boldsymbol{W}_m,1,\beta_\ell) + \sigma_R^2||\boldsymbol{W}_m||^2] \leq \bar{P}_R, m\in\mathcal{M}, \tag{44e}$$

$$(1-\tau)\tau\sum_{m\in\mathcal{M}}(\sum_{\ell\in\mathcal{K}} \Phi_{\ell,m}(\boldsymbol{W}_m,1,\beta_\ell) + \sigma_R^2||\boldsymbol{W}_m||^2) \leq P^{R,\max}_{\rm sum}. \tag{44f}$$

In contrast to the power constraints (19e) and (19f), which are convex, the last constraints (44e) and (44f) are no longer convex due to the presence of the new time fraction variable τ, which also makes the objective function in (44a) much more complex compared to that in (19a). To address (44) properly we now provide a new variable transformation to transform (19e) and (19f) to convex constraints, preserving the convexity of constraints (44b)-(44d) and even making the objective function in (44a) more computationally tractable, for which we will provide a new bounding technique. To this end, recalling the definition (17), rewrite (44d)-(44f) by

$$\sum_{k\in\mathcal{K}} 1/\sqrt{\beta_k} \leq P^{U,\max}_{\rm sum}/\tau,$$

$$\sum_{\ell\in\mathcal{K}} \Phi_{\ell,m}(\boldsymbol{W}_m,1,\beta_\ell) + \sigma_R^2||\boldsymbol{W}_m||^2 \leq \bar{P}_R/\tau,\ m\in\mathcal{M},$$

$$\sum_{m\in\mathcal{M}}\left(\sum_{\ell\in\mathcal{K}} \Phi_{\ell,m}(\boldsymbol{W}_m,1,\beta_\ell) + \sigma_R^2||\boldsymbol{W}_m||^2\right) \leq P^{R,\max}_{\rm sum}/(1-\tau)\tau.$$

Introduce the new variables $t_1>0$ and $t_2>0$ to express $1/\tau^2$ and $1/(1-\tau)$, which satisfy the convex constraint

$$1/\sqrt{t_1} + 1/t_2 \leq 1. \tag{45}$$

Then, (44) is equivalent to

$$\max_{\boldsymbol{W}\in\mathcal{C}^{N\times N},t_1,t_2\atop \boldsymbol{\alpha}\in\mathcal{R}_+^{2K},\boldsymbol{\beta}\in\mathcal{R}_+^{2K}} \quad \varphi(\boldsymbol{W},\boldsymbol{\alpha},\boldsymbol{\beta},t_2) \triangleq$$

$$\min_{k=1,\ldots,K}(1/t_2)\left[\ln\left(1+|\mathcal{L}_{k,a(k)}(\boldsymbol{W})|^2/\sqrt{\alpha_k\beta_{a(k)}}\right) + \ln\left(1+|\mathcal{L}_{a(k),k}(\boldsymbol{W})|^2/\sqrt{\alpha_{a(k)}\beta_k}\right)\right] \tag{46a}$$

$$\text{s.t.} \quad \sum_{\ell\in\mathcal{K}\setminus\{k,a(k)\}} \Psi_{k,\ell}(\boldsymbol{W},\alpha_k,\beta_\ell) + \sigma_R^2\Upsilon_k(\boldsymbol{W},\alpha_k) + \sigma_k^2/\tau\sqrt{\alpha_k} \leq 1, \tag{46b}$$

$$\beta_k \geq 1/(\bar{P}_{\rm UE})^2, k\in\mathcal{K}, \tag{46c}$$

$$\sum_{k\in\mathcal{K}} 1/\sqrt{\beta_k} \leq P^{U,\max}_{\rm sum}\sqrt{t_1}, \tag{46d}$$

$$\sum_{\ell\in\mathcal{K}} \Phi_{\ell,m}(\boldsymbol{W}_m,1,\beta_\ell) + \sigma_R^2||\boldsymbol{W}_m||^2 \leq \bar{P}_R\sqrt{t_1}, \quad m\in\mathcal{M}, \tag{46e}$$

$$\frac{1}{\sqrt{t_1}}\sum_{m\in\mathcal{M}}\left(\sum_{\ell\in\mathcal{K}} \Phi_{\ell,m}(\boldsymbol{W}_m,1,\beta_\ell) + \sigma_R^2||\boldsymbol{W}_m||^2\right) \leq t_2P^{R,\max}_{\rm sum}, \tag{46f}$$

where all constraints (46b)-(46f) are convex. Therefore, the next step is to approximate the objective function in (46a).

Suppose $(\boldsymbol{W}^{(\kappa)},\boldsymbol{\alpha}^{(\kappa)},\boldsymbol{\beta}^{(\kappa)},t_1^{(\kappa)},t_2^{(\kappa)})$ is a feasible point for (46) found at the $(\kappa-1)$th iteration. Applying (58) in the Appendix for

$$x = 1/|\mathcal{L}_{k,a(k)}(\boldsymbol{W})|^2, y = \sqrt{\alpha_k\beta_{a(k)}}, t = t_2$$

and

$$\bar{x} = 1/|\mathcal{L}_{k,a(k)}(\boldsymbol{W}^{(\kappa)})|^2, \bar{y} = \sqrt{\alpha_k^{(\kappa)}\beta_{a(k)}^{(\kappa)}}, \bar{t} = t_2^{(\kappa)}$$

and using inequality (23) yields

$$(1/t_2)\ln\left(1|\mathcal{L}_{k,a(k)}(\boldsymbol{W})|^2/\sqrt{\alpha_k\beta_{a(k)}}\right) \quad \geq$$

$$\Gamma_{k,a(k)}^{(\kappa)}(\boldsymbol{W},\alpha_k,\beta_{a(k)},t_2) \quad (47)$$

over the trust region (21), for

$$\begin{aligned} x_{k,a(k)}^{(\kappa)} &= |\mathcal{L}_{k,a(k)}(\boldsymbol{W}^{(\kappa)})|^2/\sqrt{\alpha_k^{(\kappa)}\beta_{a(k)}^{(\kappa)}} \\ c_{k,a(k)}^{(\kappa)} &= (2/t_2^{(\kappa)})\ln\left(1+x_{k,a(k)}^{(\kappa)}\right)>0, \\ d_{k,a(k)}^{(\kappa)} &= x_{k,a(k)}^{(\kappa)}/(x_{k,a(k)}^{(\kappa)}+1)t_2^{(\kappa)}>0, \\ e_{k,a(k)}^{(\kappa)} &= (1/t_2^{(\kappa)})^2\ln\left(1+x_{k,a(k)}^{(\kappa)}\right)>0, \end{aligned}$$

and

$$\begin{aligned} \Gamma_{k,a(k)}^{(\kappa)}(\boldsymbol{W},\alpha_k,\beta_{a(k)},t_2) &\triangleq \\ c_{k,a(k)}^{(\kappa)}+d_{k,a(k)}^{(\kappa)}&\left[2-\right. \\ \frac{|\mathcal{L}_{k,a(k)}(\boldsymbol{W}^{(\kappa)})|^2}{2\Re\{\mathcal{L}_{k,a(k)}(\boldsymbol{W})(\mathcal{L}_{k,a(k)}(\boldsymbol{W}^{(\kappa)}))^*\}-|\mathcal{L}_{k,a(k)}(\boldsymbol{W}^{(\kappa)})|^2}& \\ \left.-\sqrt{\alpha_k\beta_{a(k)}}/\sqrt{\alpha_k^{(\kappa)}\beta_{a(k)}^{(\kappa)}}\right]&-e_{k,a(k)}^{(\kappa)}t_2. \quad (48) \end{aligned}$$

By Algorithm 3 we propose a path-following procedure for computing (46), which solves the following convex optimization problem at the κth iteration to generate the next feasible point $(\boldsymbol{W}^{(\kappa+1)},\boldsymbol{\alpha}^{(\kappa+1)},\boldsymbol{\beta}^{(\kappa+1)},t_1^{(\kappa+1)},t_2^{(\kappa+1)})$:

$$\begin{aligned} \max_{\substack{\boldsymbol{W},\boldsymbol{\alpha},\\ \boldsymbol{\beta},t_1,t_2}} \quad & \min_{k=1,\ldots,K}\left[G_{k,a(k)}^{(\kappa)}(\boldsymbol{W},\alpha_k,\beta_{a(k)},t_1,t_2)\right. \\ & \left.+G_{a(k),k}^{(\kappa)}(\boldsymbol{W},\alpha_{a(k)},\beta_k,t_1,t_2)\right] \\ \text{s.t.} \quad & (45),(46b),(46c),(46d),(46e),(46f),(21). \quad (49) \end{aligned}$$

Analogously to Algorithm 1, the sequence $\{(\boldsymbol{W}^{(\kappa)},\boldsymbol{\alpha}^{(\kappa)},\boldsymbol{\beta}^{(\kappa)},t_1^{(\kappa)},t_2^{(\kappa)})\}$ generated by Algorithm 3 at least converges to a local optimal solution of (46).

Algorithm 3 Path-following algorithm for TF-wise HD TWR exchange throughput optimization

initialization: Set $\kappa=0$. Initialize a feasible point $(\boldsymbol{W}^{(0)},\boldsymbol{\alpha}^{(0)},\boldsymbol{\beta}^{(0)},t_1^{(0)},t_2^{(0)}))$ for the convex constraints (46b)-(46f) and $R_1=\varphi(\boldsymbol{W}^{(0)},\boldsymbol{\alpha}^{(0)},\boldsymbol{\beta}^{(0)},t_2^{(0)})$.

repeat

- $R_0=R_1$.
- Solve the convex optimization problem (49) to obtain the solution $(\boldsymbol{W}^{(\kappa+1)},\boldsymbol{\alpha}^{(\kappa+1)},\boldsymbol{\beta}^{(\kappa+1)},t_1^{(\kappa+1)},t_2^{(\kappa+1)})$.
- Update $R_1=\varphi(\boldsymbol{W}^{(\kappa+1)},\boldsymbol{\alpha}^{(\kappa+1)},\boldsymbol{\beta}^{(\kappa+1)},t_2^{(\kappa+1)})$.
- Reset $\kappa\to\kappa+1$.

until $\frac{R_1-R_0}{R_0}\le\epsilon$ for given tolerance $\epsilon>0$.

B. TF-wise HD TWR energy-efficiency maximization

Similarly to (46), problem (43) of TF-wise HD TWR energy efficiency can be equivalently expressed by

$$\max_{\boldsymbol{W},t_1,t_2,\boldsymbol{\alpha},\boldsymbol{\beta}} \quad \Theta(\boldsymbol{W},\boldsymbol{\beta},t_2) \quad (50a)$$

$$\begin{aligned} \text{s.t.} \quad & (46b),(46c),(46d),(46e),(46f), \quad (50b) \\ & \ln\left(1+|\mathcal{L}_{k,a(k)}(\boldsymbol{W})|^2/\sqrt{\alpha_k\beta_{a(k)}}\right) \\ & +\ln\left(1+|\mathcal{L}_{a(k),k}(\boldsymbol{W})|^2/\sqrt{\alpha_{a(k)}\beta_k}\right)\ge t_2r_k, \quad (50c) \end{aligned}$$

$$k=1,\cdots,K,$$

where

$$\begin{aligned} \Theta(\boldsymbol{W},\boldsymbol{\beta},t_2) \triangleq \sum_{k=1}^{K}&\left[\ln(1+\frac{|\mathcal{L}_{k,a(k)}(\boldsymbol{W})|^2}{\sqrt{\alpha_k\beta_{a(k)}}})\right. \\ &\left.+\ln(1+\frac{|\mathcal{L}_{a(k),k}(\boldsymbol{W})|^2}{\sqrt{\alpha_{a(k)}\beta_k}})\right]/t_2\pi(\boldsymbol{\beta},\boldsymbol{W},t_1) \end{aligned}$$

with the consumption power function $\pi(\boldsymbol{\beta},\boldsymbol{W})$ defined by

$$\begin{aligned} \pi(\boldsymbol{\beta},\boldsymbol{W},t_1)\triangleq& \\ \zeta\left[\sum_{k\in\mathcal{K}}\frac{1}{\sqrt{\beta_kt_1}}+(1-\frac{1}{\sqrt{t_1}})\sum_{m\in\mathcal{M}}(\sum_{\ell\in\mathcal{K}}\Phi_{\ell,m}(\boldsymbol{W}_m,1,\beta_\ell)\right.& \\ \left.+\sigma_R^2||\boldsymbol{W}_m||^2/\sqrt{t_1})\right]+MP^{\mathrm{R}}+2KP^{\mathrm{U}}.& \quad (51) \end{aligned}$$

Using the inequalities

$$\begin{aligned} \Phi_{\ell,m}(\boldsymbol{W}_m,1,\beta_\ell)/\sqrt{t_1} \ge& \\ \Phi_{\ell,m}(\boldsymbol{W}_m^{(\kappa)},1,\beta_\ell^{(\kappa)})/\sqrt{t_1^{(\kappa)}}& \\ +2\langle(\boldsymbol{W}_m^{(\kappa)})^H\boldsymbol{h}_{\ell,m}\boldsymbol{h}_{\ell,m}^H,\boldsymbol{W}_m-\boldsymbol{W}_m^{(\kappa)}\rangle/\sqrt{\beta_\ell^{(\kappa)}t_1^{(\kappa)}}& \\ -\Phi_{\ell,m}(\boldsymbol{W}_m^{(\kappa)},1,\beta_\ell^{(\kappa)})(t_1-t_1^{(\kappa)})/2(t_1^{(\kappa)})^{3/2}& \\ -(\beta_\ell-\beta_\ell^{(\kappa)})||\boldsymbol{h}_{\ell,m}^H\boldsymbol{W}_m^{(\kappa)}||^2/2\sqrt{t_1^{(\kappa)}}(\beta_\ell^{(\kappa)})^{3/2}& \end{aligned}$$

and

$$\begin{aligned} \frac{||\boldsymbol{W}_m||^2}{t_1} \ge& \frac{||\boldsymbol{W}_m^{(\kappa)}||^2}{t_1^{(\kappa)}}+2\langle\frac{\boldsymbol{W}_m^{(\kappa)}}{t_1^{(\kappa)}},\boldsymbol{W}_m-\boldsymbol{W}_m^{(\kappa)}\rangle \\ &-\frac{||\boldsymbol{W}_m^{(\kappa)}||^2}{(t_1^{(\kappa)})^2}(t_1-t_1^{(\kappa)}) \end{aligned}$$

which follow from the convexity of functions defined in (17), one can obtain

$$\pi(\boldsymbol{\beta},\boldsymbol{W},t_1)\le\pi^{(\kappa)}(\boldsymbol{\beta},\boldsymbol{W},t_1) \quad (52)$$

where

$$\begin{aligned} \pi^{(\kappa)}(\boldsymbol{\beta},\boldsymbol{W},t_1) \triangleq& \\ \zeta\left[\sum_{k\in\mathcal{K}}\frac{1}{\sqrt{\beta_kt_1}}+\sum_{m\in\mathcal{M}}\left(\sum_{\ell\in\mathcal{K}}\Phi_{\ell,m}(\boldsymbol{W}_m,1,\beta_\ell)\right.\right.& \\ \left.+\sigma_R^2\frac{||\boldsymbol{W}_m||^2}{\sqrt{t_1}}\right)-\sum_{m\in\mathcal{M}}\sum_{\ell\in\mathcal{K}}(\frac{\Phi_{\ell,m}(\boldsymbol{W}_m^{(\kappa)},1,\beta_\ell^{(\kappa)})}{\sqrt{t_1^{(\kappa)}}}& \\ +2\langle\frac{(\boldsymbol{W}_m^{(\kappa)})^H\boldsymbol{h}_{\ell,m}\boldsymbol{h}_{\ell,m}^H}{\sqrt{\beta_\ell^{(\kappa)}t_1^{(\kappa)}}},\boldsymbol{W}_m-\boldsymbol{W}_m^{(\kappa)}\rangle& \\ -\frac{\Phi_{\ell,m}(\boldsymbol{W}_m^{(\kappa)},1,\beta_\ell^{(\kappa)})}{2(t_1^{(\kappa)})^{3/2}}(t_1-t_1^{(\kappa)})& \\ -\frac{||\boldsymbol{h}_{\ell,m}^H\boldsymbol{W}_m^{(\kappa)}||^2}{2\sqrt{t_1^{(\kappa)}}(\beta_\ell^{(\kappa)})^{3/2}}(\beta_\ell-\beta_\ell^{(\kappa)})& \\ -\sum_{m\in\mathcal{M}}\sigma_R^2(\frac{||\boldsymbol{W}_m^{(\kappa)}||^2}{t_1^{(\kappa)}}+2\langle\frac{\boldsymbol{W}_m^{(\kappa)}}{t_1^{(\kappa)}},\boldsymbol{W}_m-\boldsymbol{W}_m^{(\kappa)}\rangle& \\ \left.-\frac{||\boldsymbol{W}_m^{(\kappa)}||^2}{(t_1^{(\kappa)})^2}(t_1-t_1^{(\kappa)}))\right]+MP^{\mathrm{R}}+2KP^{\mathrm{U}},& \end{aligned}$$

which is a convex function.

Suppose that $(\boldsymbol{W}^{(\kappa)}, \boldsymbol{\alpha}^{(\kappa)}, \boldsymbol{\beta}^{(\kappa)}, t_1^{(\kappa)}, t_2^{(\kappa)})$ is a feasible point for (50) found from the $(\kappa-1)$th iteration. Applying inequality (61) in the Appendix for

$$x = 1/|\mathcal{L}_{k,a(k)}(\boldsymbol{W})|^2, y = \sqrt{\alpha_k \beta_{a(k)}}, \\ z = \pi(\boldsymbol{\beta}, \boldsymbol{W}, t_1), t = t_2$$

and

$$\bar{x} = 1/|\mathcal{L}_{k,a(k)}(\boldsymbol{W}^{(\kappa)})|^2, \bar{y} = \sqrt{\alpha_k^{(\kappa)} \beta_{a(k)}^{(\kappa)}}, \\ \bar{z} = \pi(\boldsymbol{\beta}^{(\kappa)}, \boldsymbol{W}^{(\kappa)}, t_1^{(\kappa)}), \bar{t} = t_2^{(\kappa)}$$

and using inequality (23) yield

$$\frac{\ln\left(1 + |\mathcal{L}_{k,a(k)}(\boldsymbol{W})|^2/\sqrt{\alpha_k \beta_{a(k)}}\right)}{t_2 \pi(\boldsymbol{\beta}, \boldsymbol{W}, t_1)} \geq \\ \tilde{F}_{k,a(k)}^{(\kappa)}(\boldsymbol{W}, \alpha_k, \boldsymbol{\beta}, t_2) \quad (53)$$

over the trust region (21) for

$$\begin{aligned} x_{k,a(k)}^{(\kappa)} &= |\mathcal{L}_{k,a(k)}(\boldsymbol{W}^{(\kappa)})|^2/\sqrt{\alpha_k^{(\kappa)} \beta_{a(k)}^{(\kappa)}}, \\ p_{k,a(k)}^{(\kappa)} &= 3\left[\ln(1 + x_{k,a(k)}^{(\kappa)})\right]/t_2^{(\kappa)} t^{(\kappa)} > 0, \\ q_{k,a(k)}^{(\kappa)} &= x_{k,a(k)}^{(\kappa)}/(x_{k,a(k)}^{(\kappa)} + 1) t_2^{(\kappa)} t^{(\kappa)} > 0, \\ r_{k,a(k)}^{(\kappa)} &= \left[\ln(1 + x_{k,a(k)}^{(\kappa)})\right]/(t_2^{(\kappa)})^2 t^{(\kappa)} > 0, \\ s_{k,a(k)}^{(\kappa)} &= \left[\ln(1 + x_{k,a(k)}^{(\kappa)})\right]/t_2^{(\kappa)} (t^{(\kappa)})^2 > 0, \end{aligned} \quad (54)$$

and

$$\tilde{F}_{k,a(k)}^{(\kappa)}(\boldsymbol{W}, \alpha_k, \boldsymbol{\beta}, t_2) \triangleq \\ p_{k,a(k)}^{(\kappa)} + q_{k,a(k)}^{(\kappa)} [2 - \\ \frac{|\mathcal{L}_{k,a(k)}(\boldsymbol{W}^{(\kappa)})|^2}{2\Re\{\mathcal{L}_{k,a(k)}(\boldsymbol{W})(\mathcal{L}_{k,a(k)}(\boldsymbol{W}^{(\kappa)}))^*\} - |\mathcal{L}_{k,a(k)}(\boldsymbol{W}^{(\kappa)})|^2} \\ - \sqrt{\alpha_k \beta_{a(k)}}/\sqrt{\alpha_k^{(\kappa)} \beta_{a(k)}^{(\kappa)}}\Big] - r_{k,a(k)}^{(\kappa)} t_2 \\ - s_{k,a(k)}^{(\kappa)} \pi^{(\kappa)}(\boldsymbol{\beta}, \boldsymbol{W}, t_1). \quad (55)$$

By Algorithm 4 we propose a path-following procedure for computing (50), which solves the following convex optimization problem at the κth iteration to generate the next feasible point $(\boldsymbol{W}^{(\kappa+1)}, \boldsymbol{\alpha}^{(\kappa+1)}, \boldsymbol{\beta}^{(\kappa+1)}, t_1^{(\kappa+1)}, t_2^{(\kappa+1)})$:

$$\max_{\substack{\boldsymbol{W}, t_1, t_2 \\ \boldsymbol{\alpha}, \boldsymbol{\beta}}} \sum_{k=1}^{K} [\tilde{F}_{k,a(k)}^{(\kappa)}(\boldsymbol{W}, \alpha_k, \boldsymbol{\beta}, t_2) \\ + \tilde{F}_{a(k),k}^{(\kappa)}(\boldsymbol{W}, \alpha_{a(k)}, \boldsymbol{\beta}, t_2)] \quad (56a)$$

$$\text{s.t.} \quad (45), (46b) - (46f), (21), \quad (56b)$$

$$f_{k,a(k)}^{(\kappa)}(\boldsymbol{W}, \alpha_k, \beta_{a(k)}) + f_{a(k),k}^{(\kappa)}(\boldsymbol{W}, \alpha_{a(k)}, \beta_k) \geq t_2 r_k, \\ k = 1, \cdots, K, \quad (56c)$$

where $f_{k,a(k)}^{(\kappa)}$ are defined from (20).

Analogously to Algorithm 1, the sequence $\{(\boldsymbol{W}^{(\kappa)}, \boldsymbol{\alpha}^{(\kappa)}, \boldsymbol{\beta}^{(\kappa)}, t_1^{(\kappa)}, t_2^{(\kappa)})\}$ generated by Algorithm 4 at least converges to a local optimal solution of (50).

An initial feasible point $(\boldsymbol{W}^{(0)}, \boldsymbol{\alpha}^{(0)}, \boldsymbol{\beta}^{(0)}, t_1^{(0)}, t_2^{(0)})$ for initializing Algorithm 4 can be found by using Algorithm 3 for computing (46), which terminates upon

$$\min_{k=1,\ldots,K} \Big[\ln\left(1 + |\mathcal{L}_{k,a(k)}(\boldsymbol{W})|^2/\sqrt{\alpha_k \beta_{a(k)}}\right) \\ + \ln\left(1 + |\mathcal{L}_{a(k),k}(\boldsymbol{W})|^2/\sqrt{\alpha_{a(k)} \beta_k}\right)\Big]/t_2 r_k \geq 1 \quad (57)$$

to satisfy (50a)-(50c).

Algorithm 4 Path-following algorithm for TF-wise HD TWR energy-efficiency optimization

initialization: Set $\kappa = 0$. Initialize a feasible point $(\boldsymbol{W}^{(0)}, \boldsymbol{\alpha}^{(0)}, \boldsymbol{\beta}^{(0)}, t_1^{(0)}, t_2^{(0)}))$ for the convex constraints (50a)-(50c) and $e_1 = \Theta(\boldsymbol{W}^{(0)}, \boldsymbol{\alpha}^{(0)}, \boldsymbol{\beta}^{(0)}, t_2^{(0)})$.

repeat

- $e_0 = e_1$.
- Solve the convex optimization problem (56) to obtain the solution $(\boldsymbol{W}^{(\kappa+1)}, \boldsymbol{\alpha}^{(\kappa+1)}, \boldsymbol{\beta}^{(\kappa+1)}, t_1^{(\kappa+1)}, t_2^{(\kappa+1)})$.
- Update $e_1 = \Theta(\boldsymbol{W}^{(\kappa+1)}, \boldsymbol{\alpha}^{(\kappa+1)}, \boldsymbol{\beta}^{(\kappa+1)}, t_2^{(\kappa+1)})$.
- Reset $\kappa \to \kappa + 1$.

until $\frac{e_1 - e_0}{e_0} \leq \epsilon$ for given tolerance $\epsilon > 0$.

IV. Numerical Results

In this section, simulation results are presented to demonstrate the advantage of the TF-wise HD TWR conisered in Section III over FD-based TWR considered in Section II and HD TWR considered in [13]. The channel $\mathbf{h}_{k,m}$ from UE ℓ to relay m and the channel $\mathbf{g}_{m,k}$ from relay m to UE k are assumed Rayleigh fading, which are modelled by independent circularly-symmetric complex Gaussian random variables with zero means and unit variances. The power of the background noises $\boldsymbol{n}_{R,m}$ at relay m and n_k at UE k are normalized to $\sigma_R^2 = \sigma_k^2 = 1$. The tolerance for the algorithms 1-4 is set as $\epsilon = 10^{-4}$. Each point of the numerical results is the average of $1,000$ random channel realizations. Other settings are: $P_{\text{sum}}^{U,\max} = KP^{U,\max}$ and $P_{\text{sum}}^{R,\max} = MP^{A,\max}/2$, where $P^{U,\max}$ and $P_{\text{sum}}^{R,\max}$ are fixed at 10 dBW and 15 dBW; the drain efficiency of power amplifier $1/\zeta$ is 40%; the circuit powers of each antenna in relay and UE are 0.97 dBW and -13 dBW. In algorithms' implementation, the convex solver CVX [28] is used to solve convex optimization problems. Also, the performance graphs are plotted against the self-interference attenuation level σ_{SI}^2 as the latter is the most decisive parameter in FD technologies.

The scenarios of $K \in \{2, 3\}$ pairs and $(M, N_R) \in \{(1, 8), (2, 4), (4, 2)\}$ are simulated.

A. Maximin exchange information throughput optimization

To confirm the negative effect of the FD SI attenuation level σ_{SI}, Fig. 3 and 4 plot the achievable minimum pair exchange throughput versus SI σ_{SI}^2 with $K \in \{2, 3\}$. For small σ_{SI} that make FD SI to the level of the background noise, the minimum pair exchange throughput achieved by FD-based TWR still enjoys the gain offered by FD as is better than that obtained by HD TWR. However, FD cannot offset for larger σ_{SI} that make FD SI larger than the background noise, so the former becomes worse than the latter. In contrast, the minimum pair exchange throughput by TF-wise HD TWR is free of FD SI and it is significantly better than that achieved by the other two. Certainly, using all antennas for separated reception and transmission in time fractions within the time unit is not

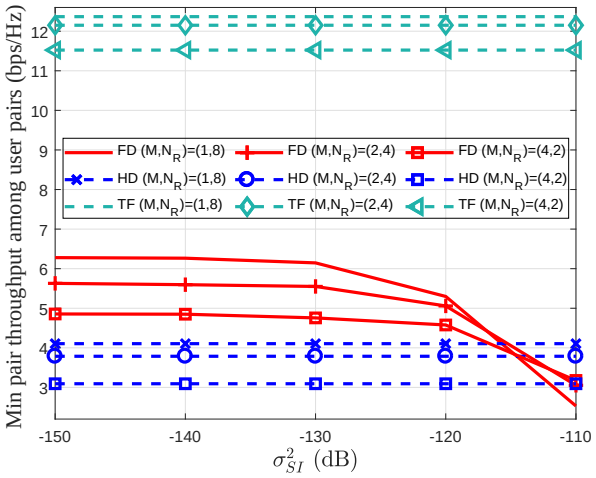

Fig. 3. Minimum pair exchange throughput versus σ_{SI}^2 with $K = 2$.

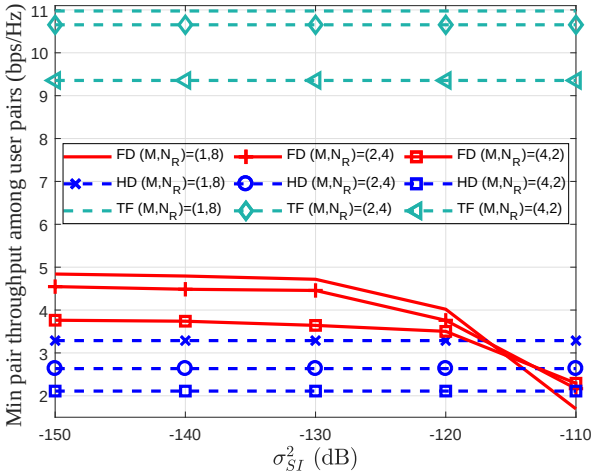

Fig. 4. Minimum pair exchange throughput versus σ_{SI}^2 with $K = 3$.

only much easier implemented but is much better than FD with simultaneous reception and transmission. It has been also shown in [29] and [30] that separated information and energy transfer in time fractions within the unit time is much more efficient and secured than the simultaneous information and energy transfer. Table I provides the achievable minimum pair exchange throughput by TF-wise HD TWR at $\tau = 0.5$, where the users use a half of a time slot to send their information to the relays and the relays use the remaining half of the time slot to send the beamformed signals to the users. Comparing with Figs. 3 and 4 reveals that TF-wise HD TWR under this not optimal time-fraction allocation still outperforms FD TWR slightly and outperforms HD TWR essentially.

Table II and III provide a computational experience in implementing Algorithm 1, which converges in less than 23 and 36 iterations in all considered FD SI scenarios for solving (14) with $K = 2$ and $K = 3$, respectively. A computational experience in implementing Algorithm 3 is provided by Table IV, which shows that Algorithm 3 converges in less than 25 iterations for solving (42) with $K = 2$ and $K = 3$.

TABLE IV
AVERAGE NUMBER OF ITERATIONS FOR COMPUTING (42) BY ALGORITHM 3.

Iterations	K=2	K=3
$(M, N_R) = (1, 8)$	23.55	22.42
$(M, N_R) = (2, 4)$	25.64	25.75
$(M, N_R) = (4, 2)$	25.32	21.43

TABLE VII
AVERAGE NUMBER OF ITERATIONS FOR COMPUTING (43) BY ALGORITHM 4.

Iterations	K=2	K=3
$(M, N_R) = (1, 8)$	20.25	19.38
$(M, N_R) = (1, 8)$	21.51	21.19
$(M, N_R) = (1, 8)$	23.13	24.08

B. EE maximization

To include a comparison with HD TWR [13], the exchange throughput threshold r_k in (15) and (43) is set as the half of the optimal value of the maximin exchange throughput optimization problem for HD TWR that is computed by [13, Alg. 1].

Fig. 5 plots the energy efficiency by the three schemes for $K = 2$. As expected, the two other schemes cannot compete with FT-wise HD TWR. The corresponding sum throughput and transmit power plotted in Figs. 6 and 7 particularly explain the superior performance of TF-wise HD TWR. The sum throughput achieved by TF-wise HD TWR is more than double that achieved by FD-based TWR and HD TWR thanks to its using more power for the relay beamforming. In contrast, Fig. 7 shows that the transmit power in FD-based TWR must be controlled to make sure that its transmission does not so severely interfere its reception. Nevertheless, FD-based TWR always achieves better EE than HD TWR in the considered range of σ_{SI}^2 though the gap becomes narrower as σ_{SI}^2. For small σ_{SI}^2, FD-based TWR achieves higher sum throughput with less transmit power as compared to HD TWR. For larger σ_{SI}^2, the former achieves almost the same sum through as the latter does but with much less transmission power, keeping its EE higher than the latter. Fig. 8 for $K = 3$ follows a similar pattern.

Lastly, Table V, VI and VII provide a computational experience in implementing Algorithm 2 for solving (15) and Algorithm 4 for solving (43). Algorithm 2 needs less than 29 and 40 iterations on average for $K = 2$ and $K = 3$, while Algorithm 4 need less than 23 and 24 iterations.

V. CONCLUSIONS

This paper has considered two possible approaches for multiple pairs of users to exchange information via multiple relays within one time slot. The first approach is based on full-duplexing (FD) at the users and relays, while the second approach is based on separated time-fraction-wise (TF-wise) half-duplexing (HD) signal transmission and reception by the users and relays. It is much easier to implement the second

TABLE I
MINIMUM PAIR EXCHANGE THROUGHPUT BY TF-WISE TWR FOR $\tau = 1/2$.

(K, M, N_R)	$(2,1,8)$	$(2,2,4)$	$(2,4,2)$	$(3,1,8)$	$(3,2,4)$	$(3,4,2)$
$\min_k R_k$	6.29	6.11	5.78	5.66	5.38	4.78

TABLE II
AVERAGE NUMBER OF ITERATIONS FOR COMPUTING (14) BY ALGORITHM 1 WITH $K = 2$.

σ_{SI}^2 (dB)	-150	-140	-130	-120	-110
$(K, M, N_R) = (2,1,8)$	13.02	14.36	13.24	15.69	18.83
$(K, M, N_R) = (2,2,4)$	18.16	17.92	16.80	17.06	19.53
$(K, M, N_R) = (2,4,2)$	23.25	18.03	21.09	19.57	21.61

TABLE III
AVERAGE NUMBER OF ITERATIONS FOR COMPUTING (14) BY ALGORITHM 1 WITH $K = 3$.

σ_{SI}^2 (dB)	-150	-140	-130	-120	-110
$(K, M, N_R) = (3,1,8)$	30.49	27.81	30.26	35.76	26.22
$(K, M, N_R) = (3,2,4)$	24.86	26.02	26.31	27.05	31.33
$(K, M, N_R) = (3,4,2)$	36.10	24.85	33.47	34.35	22.96

TABLE V
AVERAGE NUMBER OF ITERATIONS FOR COMPUTING (15) BY ALGORITHM 3 WITH $K = 2$.

σ_{SI}^2 (dB)	-150	-140	-130	-120	-110
$(K, M, N_R) = (2,1,8)$	24.85	26.18	21.02	26.63	29.43
$(K, M, N_R) = (2,2,4)$	26.49	27.76	26.04	24.18	27.09
$(K, M, N_R) = (2,4,2)$	23.87	23.24	24.31	24.65	22.83

TABLE VI
AVERAGE NUMBER OF ITERATIONS FOR SOLVING (15) BY ALGORITHM 3 WITH $K = 3$.

σ_{SI}^2 (dB)	-150	-140	-130	-120	-110
$(K, M, N_R) = (3,1,8)$	29.40	28.59	30.42	37.31	40.46
$(K, M, N_R) = (3,2,4)$	27.81	28.17	30.65	32.45	31.19
$(K, M, N_R) = (3,4,2)$	31.75	24.44	26.13	25.37	30.38

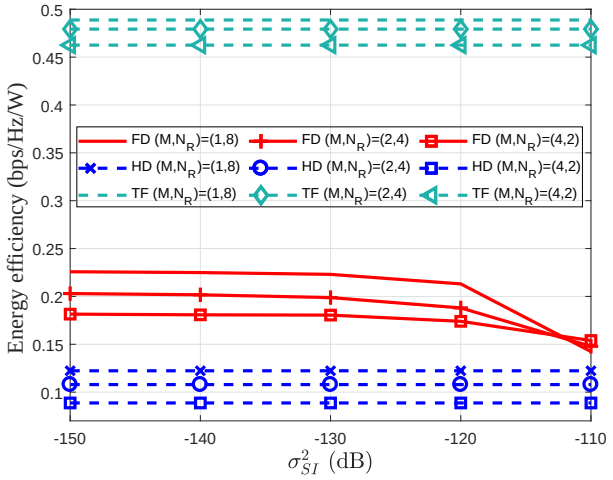

Fig. 5. Energy efficiency versus σ_{SI}^2 with $K = 2$.

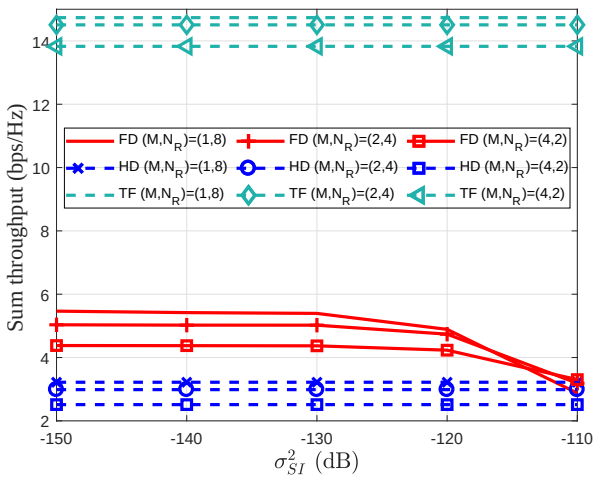

Fig. 6. Sum thoughput versus σ_{SI}^2 with $K = 2$.

approach than the first approach. In order to compare their capability, we have considered two fundamental problems of joint design of UE power allocation and relay beamforming to optimize the spectral efficiency and energy efficiency. Path-following optimization algorithms have been devised for their computation. Simulation results have confirmed their rapid convergence. TF-wise HD TWR has been shown to easily outperform FD-based TWR and HD TWR. The throughput of a network is not only dependent on the bandwidth but is dependent on the transmit power and interference and noise.

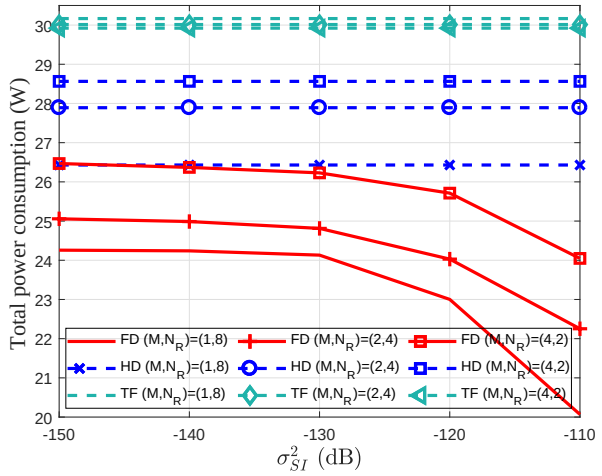

Fig. 7. Total power versus σ^2_{SI} with $K = 2$.

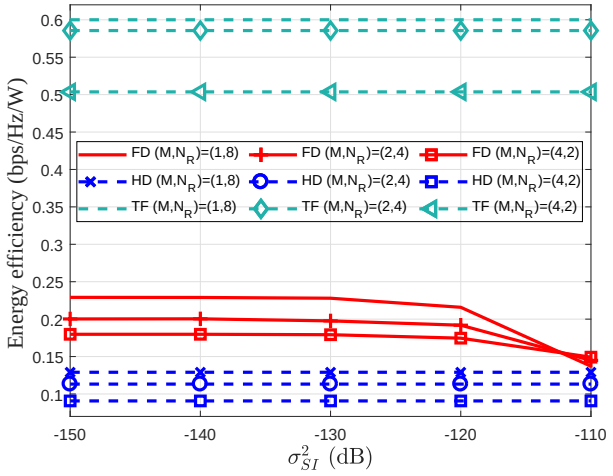

Fig. 8. Energy efficiency versus σ^2_{SI} with $K = 3$.

Certainly, one does not need to double bandwidth to achieve the same throughput within a half time slot, but one needs to manage the transmit power and interference, as our proposed TF-based approach particularly shows. Additionally, the TF-based approach could explore more the relay's diversity as it enables to use all relay antennas for receiving and transmitting signals that really helps to improve the network throughput. Some important issues such as how they work under decode-and-forward relaying are certainly of our future considerations.

APPENDIX

Let $\mathbb{R}^N_+ \triangleq \{(x_1, \ldots, x_N) : \ x_i > 0, \ i = 1, 2, \ldots, N\}$ and $\mathbb{R}_+ \triangleq (0, +\infty)$. In [31], it was proved that function $\psi(x, y, t) = (\ln(1 + 1/xy))/t$ is convex on $\mathbb{R}^3_+$. Therefore [32]

$$\begin{aligned}\frac{\ln(1+1/xy)}{t} &= \psi(x,y,t)\\ &\geq \psi(\bar{x},\bar{y},\bar{t})\\ &\quad +\langle\nabla\psi(\bar{x},\bar{y},\bar{t}),(x,y,t)-(\bar{x},\bar{y},\bar{t})\rangle\\ &= 2\frac{\ln(1+1/\bar{x}\bar{y})}{\bar{t}}+\frac{1}{(\bar{x}\bar{y}+1)\bar{t}}(2-\frac{x}{\bar{x}}-\frac{y}{\bar{y}})\\ &\quad -\frac{\ln(1+1/\bar{x}\bar{y})}{\bar{t}^2}t \qquad (58)\\ &\quad \forall\ (x,y,t)\in\mathbb{R}^3_+,(\bar{x},\bar{y},\bar{t})\in\mathbb{R}^3_+.\end{aligned}$$

The right-hand-side (RHS) of (58) agrees with the left-hand-side (LHS) at $(\bar{x}, \bar{y}, \bar{t})$.
Particularly,

$$\begin{aligned}\ln(1+1/xy) \geq 2\ln(1+1/\bar{x}\bar{y})+\frac{1}{(\bar{x}\bar{y}+1)}(2-\frac{x}{\bar{x}}-\frac{y}{\bar{y}})\\ \forall\ (x,y)\in\mathbb{R}^2_+,(\bar{x},\bar{y})\in\mathbb{R}^2_+. \qquad (59)\end{aligned}$$

Lemma 1: If function $f(\mathbf{x}, t)$ is convex in $\mathbf{x}$ and $t \in \mathbb{R}_+$ and also is decreased in t then function $f(\mathbf{x}, \sqrt{yz})$ is convex in $\mathbf{x}$ and $(y, z) \in \mathbb{R}^2_+$.
Proof: Since $\sqrt{yz}$ is a concave function, it is true that

$$\begin{aligned}\sqrt{(\alpha y_1+\beta y_2)(\alpha_1 z_1+\alpha_2 z_2)}\geq\alpha_1\sqrt{y_1z_1}+\alpha_2\sqrt{y_2z_2}\\ \forall\ \alpha_i\geq 0,\alpha_1+\alpha_2=1,y_i\geq 0,z_i\geq 0,i=1,2.\end{aligned}$$

Therefore

$$\begin{aligned}&f(\alpha_1\mathbf{x}_1+\alpha_2\mathbf{x}_2,\sqrt{(\alpha_1y_1+\alpha_2y_2)(\alpha_1z_1+\alpha_2z_2)})\\ \leq\ &f(\alpha_1\mathbf{x}_1+\alpha_2\mathbf{x}_2,\alpha_1\sqrt{y_1z_1}+\alpha_2\sqrt{y_2z_2})\\ \leq\ &\alpha_1 f(\mathbf{x}_1,\sqrt{y_1z_1})+\alpha_2 f(\mathbf{x}_2,\sqrt{y_2z_2}),\end{aligned}$$

showing the convexity of $f(\mathbf{x}, \sqrt{yz})$.
Lemma 2: Function $f(x, y, t) = (\ln(1+1/xy))/t^2$ is convex on $\mathbb{R}^3_+$.
Proof: One has

$$\begin{aligned}&\nabla^2 f(x,y,t)\\ =\ &\begin{bmatrix}\frac{2xy+1}{x^2(xy+1)^2t^2} & \frac{1}{(xy+1)^2t^2} & \frac{2}{t^3(xy+1)x}\\ \frac{1}{(xy+1)^2t^2} & \frac{2xy+1}{y^2(xy+1)^2t^2} & \frac{2}{t^3(xy+1)y}\\ \frac{2}{t^3(xy+1)x} & \frac{2}{t^3(xy+1)y} & \frac{6\ln(1+1/xy)}{t^4}\end{bmatrix}\\ \succeq\ &(x^2y^2(xy+1)^2t^4)^{-1}\\ &\begin{bmatrix}(2xy+1)y^2t^2 & x^2y^2t^2 & 2t(xy+1)xy^2\\ x^2y^2t^2 & (2xy+1)x^2t^2 & 2t(xy+1)x^2y\\ 2t(xy+1)xy^2 & 2t(xy+1)x^2y & 6(xy+1)x^2y^2\end{bmatrix},\end{aligned} \qquad (60)$$

because $\ln(1 + 1/t) \geq 1/(t + 1) \quad \forall\ t > 0$ [31, Lemma 1]. Here and after $\mathbf{A} \succeq \mathbf{B}$ for real symmetric matrices $\mathbf{A}$ and $\mathbf{B}$ means that $\mathbf{A} - \mathbf{B}$ is positive definite.

Then, calculating the subdeterminants of the matrix in the RHS of (60) yields

$$\begin{aligned}(2xy+1)y^2t^2>0,\\ \begin{vmatrix}(2xy+1)y^2t^2 & x^2y^2t^2\\ x^2y^2t^2 & (2xy+1)x^2t^2\end{vmatrix}=\\ x^2y^2t^4(3x^2y^2+4xy+1)>0,\end{aligned}$$

and

$$\begin{aligned}\begin{vmatrix}(2xy+1)y^2t^2 & x^2y^2t^2 & 2t(xy+1)xy^2\\ x^2y^2t^2 & (2xy+1)x^2t^2 & 2t(xy+1)x^2y\\ 2t(xy+1)xy^2 & 2t(xy+1)x^2y & 6(xy+1)x^2y^2\end{vmatrix}=\\ 12(xy+1)^2x^5y^5t^4>0.\end{aligned}$$

Therefore the matrix in the RHS of (60) is positive definite, implying that the Hessian $\nabla^2 f(x,y,t)$ is positive definite too, which is the necessary and sufficient condition for the convexity of f [32]. □

By applying Lemma 2 and Lemma 1, function $\psi(x,y,z,t) = (\ln(1+1/xy))/zt$ is convex on $\mathbb{R}^4_+$. Therefore, for all $(x,y,z,t) \in \mathbb{R}^4_+$, and $(\bar{x},\bar{y},\bar{z},\bar{t}) \in \mathbb{R}^4_+$, it is true that [32]

$$\begin{aligned}
\frac{\ln(1+1/xy)}{zt} &= \\
\psi(x,y,z,t) &\geq \\
\psi(\bar{x},\bar{y},\bar{z},\bar{t}) + \langle \nabla\psi(\bar{x},\bar{y},\bar{z},\bar{t}), (x,y,z,t) - (\bar{x},\bar{y},\bar{z},\bar{t})\rangle &= \\
3\frac{\ln(1+1/\bar{x}\bar{y})}{\bar{z}\bar{t}} + \frac{1}{(\bar{x}\bar{y}+1)\bar{z}\bar{t}}(2 - \frac{x}{\bar{x}} - \frac{y}{\bar{y}}) & \\
-\frac{\ln(1+1/\bar{x}\bar{y})}{\bar{z}^2\bar{t}}z - \frac{\ln(1+1/\bar{x}\bar{y})}{\bar{z}\bar{t}^2}t & \quad (61)
\end{aligned}$$

REFERENCES

[1] Y.-S. Choi and H. Shirani-Mehr, "Simultaneous transmission and reception: algorithms, design and system level performance," *IEEE Trans. Wirel. Commun.*, vol. 12, pp. 5992–6010, Dec. 2013.

[2] S. Hong, J. Brand, J. I. Choi, J. Mehlman, S. Katti, and P. Levis, "Application of self-interference cancellation in 5G and beyond," *IEEE Commun. Mag.*, vol. 52, pp. 114–21, Feb. 2014.

[3] E. Everett, A. Sahai, and A. Sabharwal, "Passive self-interference suppression for full-duplex infrastructure nodes," *IEEE Trans. Wirel. Commun.*, vol. 13, pp. 680–694, Feb. 2014.

[4] V. Syrjala, M. Valkama, L. Anttila, T. Riihonen, and D. Korpi, "Analysis of oscillator phase-noise effects on self-interference cancellation in full-duplex OFDM radio trancseivers," *IEEE Trans. on Wireless Commun.*, vol. 13, pp. 2977–2990, Jun. 2014.

[5] W. Li and R. D. Murch, "An investigation into baseband techniques for single-channel full duplex wireless communication systems," *IEEE Trans. on Wireless Commun.*, vol. 13, pp. 4794–4806, Sep. 2014.

[6] B. Rankov and A. Wittneben, "Spectral efficient protocols for half-duplex fading relay channels," *IEEE J. Select. Areas in Commun.*, vol. 25, pp. 379–389, Feb. 2007.

[7] G. Amarasuriya, C. Tellambura, and M. Ardakani, "Two-way amplify-and-forward multiple-input multiple-output relay networks with antenna selection," *IEEE J. Select. Areas Commun.*, vol. 30, pp. 1513–1529, Sep. 2012.

[8] H. Chung, N. Lee, B. Shim, and T. Oh, "On the beamforming design for MIMO multipair two-way relay channels," *IEEE Trans. Vehicular Technology*, vol. 16, pp. 3301–3306, Sep. 2012.

[9] D. Gunduz, A. Yener, A. Goldsmith, and H. V. Poor, "The multiway relay channel," *IEEE Trans. Inf. Theory*, vol. 59, pp. 51–63, Jan 2013.

[10] H. D. Tuan, D. T. Ngo, and H. H. M. Tam, "Joint power allocation for MIMO-OFDM full-duplex relaying communications," *EURASIP J. Wirel. Commun. Networking*, 2017, DOI 10.1186/s13638-016-0800-4.

[11] R. Zhang, Y.-C. Liang, C. C. Chai, and S. Cui, "Optimal beamforming for two-way multi-antenna relay channel with analogue network coding," *IEEE J. Select. Areas Commun.*, vol. 27, pp. 699–712, Jul. 2009.

[12] M. Zeng, R. Zhang, and S. Cui, "On design of collaborative beamforming for two-way relay networks," *IEEE Trans Signal Process.*, vol. 59, pp. 2284–2295, May 2011.

[13] Z. Sheng, H. D. Tuan, T. Q. Duong, and H. V. Poor, "Joint power allocation and beamforming for energy-efficient two-way multi-relay communications," *IEEE Trans. Wirel. Commun.*, vol. 16, pp. 6660–6671, Oct. 2017.

[14] A. Asadi, Q. Wang, and V. Mancuso, "A survey device-to-device communication in cellular networks," *IEEE Commun. Surveys & Tut.*, vol. 16, pp. 1801–1819, 4th Qart. 2014.

[15] J. Liu, N. Kato, J. Ma, and N. Kadowaki, "Device-to-device communication in LTE-advanced networks: A survey," *IEEE Commun. Surveys Tuts.*, vol. 17, pp. 1923–1940, 4th Quart. 2015.

[16] "2020: Beyond 4G radio evelution for the gigabit experience," *White paper, Nokia Siemens Networks*, 2011.

[17] H. Ji et al., "Overview of full-dimension MIMO in LTE- advanced pro," *IEEE Commun. Mag.*, vol. 55, pp. 176–184, Feb. 2017.

[18] P. Schulz et al., "Latency critical IoT applications in 5G: Perspective on the design of radio interface and network architecture," *IEEE Commun. Mag.*, vol. 55, pp. 70–78, Feb. 2017.

[19] H. H. M. Tam, H. D. Tuan, and D. T. Ngo, "Successive convex quadratic programming for quality-of-service management in full-duplex MU-MIMO multicell networks," *IEEE Trans. Comm.*, vol. 64, pp. 2340–2353, Jun. 2016.

[20] Z. Sheng, H. D. Tuan, H. H. M. Tam, H. H. Nguyen, and Y. Fang, "Energy-efficient precoding in multicell networks with full-duplex base stations," *EURASIP J. Wirel. Commun. Networking*, 2017, DOI 10.1186/s13638-017-0831-5.

[21] B. K. Chalise and L. Vandendorpe, "Optimization of MIMO relays for multipoint-to-multipoint communications: Nonrobust and robust designs," *IEEE Trans. Signal Process.*, vol. 58, pp. 6355–6368, Dec. 2010.

[22] A. H. Phan, H. D. Tuan, H. H. Kha, and H. H. Nguyen, "Iterative D.C. optimization of precoding in wireless MIMO relaying," *IEEE Trans. Wirel. Commun.*, vol. 12, pp. 1617–1627, Apr. 2013.

[23] S. Buzzi, C.-L. I, T. E. Klein, H. V. Poor, C. Yang, and A. Zappone, "A survey of energy-efficient techniques for 5G networks and challenges ahead," *IEEE J. Select. Areas Commun.*, vol. 34, pp. 697–709, Apr. 2016.

[24] A. Zappone, L. Sanguinetti, G. Bacci, E. A. Jorswieck, and M. Debbah, "Energy-efficient power control: A look at 5G wirel. technologies," *IEEE Trans. Signal Process.*, vol. 64, pp. 1668–1683, Apr. 2016.

[25] B. Dacorogna and P. Marechal, "The role of perspective functions in convexity, polyconvexity, rank-one convexity and separate convexity," *J. of Convex Analysis*, vol. 15, no. 2, pp. 271–284, 2008.

[26] H. H. Kha, H. D. Tuan, H. H. Nguyen, and H. H. M. Tam, "Joint design of user power allocation and relay beamforming in two-way mimo relay networks," in *Proc. 7th Inter. Conf. Signal Process. Commun. Syst. (ICSPCS)*, pp. 1–6, 2013.

[27] B. R. Marks and G. P. Wright, "A general inner approximation algorithm for nonconvex mathematical programms," *Operations Research*, vol. 26, pp. 681–683, Jul. 1978.

[28] M. Grant and S. Boyd, "CVX: Matlab software for disciplined convex programming, version 2.1." http://cvxr.com/cvx, Mar. 2014.

[29] A. A. Nasir, H. D. Tuan, D. T. Ngo, T. Q. Duong, and H. V. Poor, "Beamforming design for wireless information and power transfer systems: Receive power-splitting vs transmit time-switching," *IEEE Trans. Commun.*, vol. 65, no. 2, pp. 876–889, 2017.

[30] A. A. Nasir, H. D. Tuan, T. Q. Duong, and H. V. Poor, "Secrecy rate beamforming for multicell networks with information and energy harvesting," *IEEE Trans. Signal Process.*, vol. 65, no. 3, pp. 677–689, 2017.

[31] Z. Sheng, H. D. Tuan, A. A. Nasir, T. Q. Duong, and H. V. Poor, "Power allocation for energy efficiency and secrecy of interference wireless networks," *IEEE Trans. Wirel. Commun.*, vol. PP, no. 99, 2018.

[32] H. Tuy, *Convex Analysis and Global Optimization (second edition)*. Springer International Publishing, 2016.

Zhichao Sheng was born in Yangzhou, China. He received the B.S. degree in communication engineering from Nanjing University of Information Science and Technology, Nanjing, China, in 2008, the M.S. degree in signal and information processing from Jiangsu University of Science and Technology, Zhenjiang, China, in 2012, and the PhD degree in Electrical Engineering from the University of Technology, Sydney, NSW, Australia, in 2018. His present research interests include optimization methods for wireless communication and signal processing.

Hoang Duong Tuan received the Diploma (Hons.) and Ph.D. degrees in applied mathematics from Odessa State University, Ukraine, in 1987 and 1991, respectively. He spent nine academic years in Japan as an Assistant Professor in the Department of Electronic-Mechanical Engineering, Nagoya University, from 1994 to 1999, and then as an Associate Professor in the Department of Electrical and Computer Engineering, Toyota Technological Institute, Nagoya, from 1999 to 2003. He was a Professor with the School of Electrical Engineering and Telecommunications, University of New South Wales, from 2003 to 2011. He is currently a Professor with the School of Electrical and Data Engineering, University of Technology Sydney. He has been involved in research with the areas of optimization, control, signal processing, wireless communication, and biomedical engineering for more than 20 years.

Trung Q. Duong (S'05, M'12, SM'13) received his Ph.D. degree in Telecommunications Systems from Blekinge Institute of Technology (BTH), Sweden in 2012. Currently, he is with Queen's University Belfast (UK), where he was a Lecturer (Assistant Professor) from 2013 to 2017 and a Reader (Associate Professor) from 2018. His current research interests include Internet of Things (IoT), wireless communications, molecular communications, and signal processing. He is the author or co-author of 290 technical papers published in scientific journals (165 articles) and presented at international conferences (125 papers).

Dr. Duong currently serves as an Editor for the IEEE TRANSACTIONS ON WIRELESS COMMUNICATIONS, IEEE TRANSACTIONS ON COMMUNICATIONS, IET COMMUNICATIONS, and a Lead Senior Editor for IEEE COMMUNICATIONS LETTERS. He was awarded the Best Paper Award at the IEEE Vehicular Technology Conference (VTC-Spring) in 2013, IEEE International Conference on Communications (ICC) 2014, IEEE Global Communications Conference (GLOBECOM) 2016, and IEEE Digital Signal Processing Conference (DSP) 2017. He is the recipient of prestigious Royal Academy of Engineering Research Fellowship (2016-2021) and has won a prestigious Newton Prize 2017.

H. Vincent Poor (S72, M77, SM82, F87) received the Ph.D. degree in EECS from Princeton University in 1977. From 1977 until 1990, he was on the faculty of the University of Illinois at Urbana-Champaign. Since 1990 he has been on the faculty at Princeton, where he is the Michael Henry Strater University Professor of Electrical Engineering. From 2006 until 2016, he served as Dean of Princetons School of Engineering and Applied Science. He has also held visiting appointments at several other institutions, including most recently at Berkeley and Cambridge. His research interests are in the areas of information theory and signal processing, and their applications in wireless networks, energy systems and related fields. Among his publications in these areas is the recent book Information Theoretic Security and Privacy of Information Systems (Cambridge University Press, 2017).

Dr. Poor is a member of the National Academy of Engineering and the National Academy of Sciences, and is a foreign member of the Chinese Academy of Sciences, the Royal Society and other national and international academies. He received the Technical Achievement and Society Awards of the IEEE Signal Processing Society in 2007 and 2011, respectively. Recent recognition of his work includes the 2017 IEEE Alexander Graham Bell Medal, Honorary Professorships from Peking University and Tsinghua University, both conferred in 2017, and a D.Sc. honoris causa from Syracuse University, awarded in 2017.

Yong Fang received the Ph.D. degree in Electronic Engineering from City University of Hong Kong, Hong Kong, in 1999. He is now a professor in the School of Communication and Information Engineering, Shanghai University, Shanghai, China. His research interests include communication signal processing, blind signal processing, and adaptive information system.